Brain circuits for the representation of subjective reward value

by

Ana Marcia Fiallos

B.S. in Computer Engineering
University of Miami, 2002

Submitted to the Department of Brain and Cognitive Sciences in partial fulfillment of the requirements for the degree of

DOCTOR OF PHILOSPHY IN SYSTEMS NEUROSCIENCE

at the

MASSACHUSETTS INSTITUTE OF TECHNOLOGY

February 2011

Signature of Author: _____
Department of Brain and Cognitive Sciences
12 October 2010

Certified by: _____
Alan Pradip Pasanoff, Ph.D.
Associate Professor of Biological Engineering
Thesis Supervisor

Accepted by: _____
Earl K. Miller, Ph.D.
Picower Professor of Neuroscience
Director, BCS Graduate Program

Abstract

Successful interaction with the external world requires choosing appropriate actions in the context of available choices. Such decisions require the evaluation of the reward magnitude, or value, associated with each potential action. Delineating the neural circuits involved in this process remains an important goal in systems neuroscience. However, little is known about the neural circuits that compute, or represent, low level primary reward signals. We have combined quantitative psychophysical measures of subjective reward magnitude elicited by rewarding electrical brain stimulation, fMRI as a readout of whole-brain neural activity, and local inactivation of brain structures, to identify the neural representation of subjective reward magnitude. We find that multiple brain regions are activated by rewarding brain stimulation, but only two brain regions, the nucleus accumbens and the central and basolateral nucleus of the amygdala, exhibit patterns of activity levels that track the reward magnitude measured psychophysically, suggesting a role in the neural representation of reward magnitude. Furthermore, pharmacological silencing of the ventral tegmental area (VTA) disrupts reward-tracking behavior and increases stimulus-dependent activity in the nucleus accumbens and amygdala. Together these data suggest that ascending and descending pathways combine to produce a signal that ultimately guides behavior and is subject to modulation by VTA inputs.

Acknowledgments

I would like to thank my advisor, Alan Jasanoff, for his support, his ideas, the teachable moments while troubleshooting our scanner, an inspiring research environment with research meetings, one-on-one lunches & journal clubs, and for interesting fellow PhD's in training that I shared an office with over the years. I'm so grateful to have sat next to my best labmate, Yuri Mastumoto, for several years. We shared so many stories, and I learned a lot about collegiate cycling! I also shared so much with other talented and extremely intelligent students, postdocs, and UROPs in our lab. I would also like to express my gratitude to my thesis committee: Mriganka Sur, Ki Goosens, and Joe Mandeville for their insights and encouragement.

I am grateful to many in the Department of Brain and Cognitive Sciences. I have made numerous life-long friendships with fellow graduate students in BCS, but in particular with those in my class. From the first day of orientation I formed an unbreakable bond with Cortina McCurry, who lived below me in the graduate dorms, and made life inside and outside of neuroscience exciting. Being a Florida girl, easily overwhelmed by snow, it was only natural that I would team up with the only Alaskan in the department! To Rosa Cao, thank you for your brutally honest friendship, tolerance, and for your vast knowledge of things neuroscience and un-neuroscience. Lena Khibnik and Sally Kwok, I enjoyed our lunches in the food court, thank you for listening and critiquing my powerpoint presentations, and for all our talks about science, publishing, life after grad school, and family. And a special thanks to denise heintze for being a wizardess of the inner workings of BCS and MIT in general; you provided so much guidance and clarity through the fuzzy and confusing journey that is grad school! I thank Suzanne Corkin who made me feel at ease and welcomed at MIT, especially during the first few months after I arrived.

I am immeasurably indebted to my husband, James Schummers, and to my family for instilling within me a strong foundation of determination and fortitude of mind. I could not have accomplished any of the successes I achieved without your support and unwavering love.

"Whatever course you decide upon, there is always someone to tell you that you are wrong. There are always difficulties arising which tempt you to believe that your critics are right. To map out a course of action and follow it to an end requires courage."

~Ralph Waldo Emerson

Table of Contents

INTRODUCTION (CHAPTER 1)

Background

Decision-making is critical for successful interaction with the world

Effective interaction with the external environment requires a continuous stream of decisions among choices for actions. Each such decision requires the assimilation of a large number of factors, including innate drives, internal states (hunger, estrous etc), previous experience (memories or associations), expectation of positive outcome (reward), negative outcome, and likelihood of success. Each of these factors is represented by specific brain systems, which thus need to be integrated before being accessed by the neural circuits responsible for decision-making (Figure 1). Given the complex nature of all of these factors in the natural world, a productive experimental approach has been to examine the principles of decision making in highly reduced experimental paradigms such as two-choice operant tasks. Research using two choice tasks has uncovered a fundamental empirical rule of decision making, formalized by Herrnstein: animals will make choices in direct proportion to the relative magnitude of reward resulting from each choice (see below). Herrnstein and others have gone on to show that this powerful rule generalizes to more complex and naturalistic environments, and across all species, including humans (Herrnstein 1974). Rewards are often complex to measure experimentally, and may be highly variable with internal state, dependent on individual preferences and memories, etc. In order to isolate primary rewards, in as pure a form as possible, we employed rewarding electrical brain stimulation (BSR). Electrical stimulation of certain structures in the brain allows experimenters to tap into the same reward circuits activated by natural rewards, in a

controlled and parametric fashion (Olds and Milner, 1954). Animals, including goldfish, rats and humans, will work vigorously to induce rewarding electrical stimulation in specific brain areas (Olds and Milner 1954; Boyd and Gardner 1962; Bishop, Elder et al. 1963).

A long history of experiments using rewarding brain stimulation (BSR) has demonstrated panoply of brain regions that elicit reward (Olds and Milner 1954). The location of many of these regions along the mesolimbic pathway has suggested that this pathway may be a key component of the brain circuitry that represents reward. Further studies showing that pharmacological manipulations of the dopamine neurotransmitter system dramatically affect the rewarding aspects of brain stimulation of mesolimbic sites have supported the notion that dopaminergic signaling plays a key role in reward processing (Franklin 1978; Koob, Le et al. 1987). However, experiments which have attempted to clarify the exact circuit, by lesioning various putative neuroanatomical components have failed to isolate the necessary and sufficient components of the circuit (Olds and Olds 1969; Boyd and Celso 1970; Waraczynski, Ton et al. 1990; Waraczynski, Perkins et al. 1999; Zahm 1999).

Defining reward

Psychologists have long been aware of the influence reward and valuations have on decision making processes. Yet arriving at a unified definition of what a "reward" is has proven difficult. This is the case primarily due to the fact that a sensory system or specific "receptor" type for rewarding stimuli has not been identified; instead, scientists most commonly define a reward operationally as a stimulus that increases the

probability of a closely antecedent behavior occurring again. Defining reward on the basis of an operational outcome has unavoidably tied the study of reward processes to motivational states. Another often used definition of a reward is a stimulus that produces pleasure. Defining reward on the basis of a subjective experience of a stimulus highlights the difficulties faced by researchers who hope to elucidate the neurobiological substrate of such a psychological construct. It is not surprising that key aspects of the brain mechanisms that underlie the evaluation of costs and benefits of available options are not understood. For the purposes of this thesis, we will use reward to refer to the operational definition of reward as a reinforcer of behavior. We will use BSR, as it represents a particularly direct and quantifiable rewarding stimulus.

Theories of dopamine function: pleasure, reward prediction, and incentive salience

Rewards are usually associated with the subjective feeling of pleasure. Rewards induce changes in observable behavior and serve as positive reinforcers by increasing the frequency of the behavior that result in reward. A popular hypothesis known as the anhedonia model states that dopamine is needed in order to experience pleasure (Wise, Spindler et al. 1978). According to the anhedonia model, dopamine release is the hedonic signal of the brain that represents the pleasure associated with a reward. However, several subsequent experiments have challenged this theory. Experiments in animals by Berridge and colleagues show that orofacial movements associated with licking sucrose are not altered by dopaminergic lesions or dopamine antagonists (Wise and Rompre 1989). Perhaps more telling are experiments using intracranial self-stimulation (ICSS) during which animals repeatedly press a lever to electrically stimulate

their own dopamine-releasing neurons. These studies show that the release of dopamine is necessary for learning the association between lever-pressing and ICSS, but dopamine release diminishes during ICSS (Garris, Kilpatrick et al. 1999). These factors point to alternative roles of dopamine in reward.

A competing theory supported by Schultz and colleagues (Schultz 1999; Schultz 2002) suggests that reward magnitudes are computed elsewhere in the brain and provide input into a reward prediction error signal encoded by neurons in the substantia nigra (SN) and the VTA. This model suggests that animals learn to predict when future rewards will occur via a prediction signal where dopaminergic neurons phasically fire during the learning of a stimulus-response (S-R) association but are generally inactive thereafter. Conversely, pharmacological inhibition and lesion studies show that depleting dopamine signaling diminishes an animal's ability to motivate behaviors towards attaining rewards even after S-R pairings are learned (Cheer, Aragona et al. 2007; Day, Roitman et al. 2007), supporting the anhedonia hypothesis. Both theories implicate dopamine in reward anticipation and reward seeking behaviors.

Rewards are now recognized to act at least as importantly as hedonic incentives, causing neural representations that elicit motivation and goal pursuit, rather than as mere habit reinforcers. The incentive salience hypothesis proposed by Berridge and Robinson states that changes in levels of dopamine release affects motivated behavior but do not change the value of rewards themselves (Berridge and Robinson 1998). They introduce the terms 'wanting' and 'liking' as a way to differentiate between motivated behavior and reward values. Incentive salience is a motivational component of reward that transforms sensory information about rewards into desired incentives. In

other words, incentive salience is the process through which dopamine transforms a stimulus into an object of attraction that an animal will work to acquire. Incentive salience or 'wanting', unlike 'liking', is influenced by dopamine transmission (Berridge and Robinson 1998). Therefore, 'wanting' may depend on different neural substrates. A number of experiments have demonstrated that activity of dorsolateral prefrontal cortex neurons is predictive of an animal's decision in behavioral choice tasks (Quintana, Yajeya et al. 1988). Recordings from neurons in the dorsolateral prefrontal cortex of monkeys show that PFC neurons respond more when the monkey expected a larger reward. It is reasonable to surmise that this modulation by the magnitude of an expected reward is dopamine dependent given that the PFC receives projections from VTA neurons.

BSR vs. Natural rewards

Previous work has shown that BSR mimics many of the properties of natural reinforcers. When rodents are presented with forced choice tests which put sucrose solutions and rewarding brain stimulation in competition, the strength of electrical stimulation can be adjusted so that the rat prefers it more, less, or equally to sucrose (Conover and Shizgal 1994). In further expanded experiments, Shizgal et al. found that sucrose and brain stimulation presented in conjunction are chosen by animals in a manner that suggests that the individual positive values attributed to each are summated. Summation is only possible if both stimuli converge on the same neural system that computes reward (Shizgal 1997). These studies indicate there is a common neural mechanism for evaluating rewards provided by natural and artificial stimuli. Therefore, BSR is a useful approach in the quest to isolate components of the neural

circuit that compute and represent reward values which later guide behaviors in the lab as well as in natural settings.

Counter Model of Reward Integration

Gallistel and colleagues have used matching behavior to characterize how the intensity of BSR grows as a function of stimulation strength (Edmonds, Stellar et al. 1974). Herrnstein's matching law states that animals allocate time or responses in direct proportion to the fraction of total rewards earned (in relation to alternative options) (Gallistel, King et al. 2007). What they have shown is that as the stimulation frequency is increased, an animal's rate of operant responding grows rapidly with increasing stimulation, but eventually reaches a an asymptote (Gallistel and Leon 1991; Gallistel, Leon et al. 1991; Simmons and Gallistel 1994). A careful series of experiments has determined the asymptote cannot be explained by limitations of neural firing at frequencies below 250Hz (Forgie and Shizgal 1993), suggesting that the saturation arises due to neural circuit phenomena. The results of matching experiments have led to the development of a model of how the utility of rewarding brain stimulation is computed and translated into behavioral allocations. The model developed by these behavioral neuroscientists describes a putative network of neurons that essentially count the number action potentials caused by BSR over a time period. The counter then translates the incoming spikes into an internal representation of the intensity of reward which is later used to determine the allocation of behavioral choices (Shizgal 1997).

The counter model describes the circuitry responsible for reward value computation (in the context of BSR) into two general components: the reward cable (the fibers directly stimulated by BSR) and the reward integrator (some unknown neural

substrate) (Gallistel 1978; Gallistel and Leon 1991). The reward cable consists of the reward relevant axons directly stimulated through an implanted electrode. The reward integrator refers to the neurophysiological processes downstream from the reward cable. The counter model proposes that the integrator determines the magnitude of the reward signal by summating the total number of action potentials produce in the reward cable (Simmons and Gallistel, 1994). Experiments show how intensity of reinforcement can be held constant by adjusting the current or frequency of stimulation in a counterbalanced fashion. A high current, low frequency train can be adjusted so that it is equally preferred to a low current, high frequency train. This trade-off can be explained by assuming that the number of reward relevant axons fired by a pulse is proportional to the current (increasing the current proportionally increases the number of axons firing). Therefore the total number of action potentials generated on the reward cable is the multiplication of the number of action potentials generated by a stimulus train (frequency) and the number of axons firing (current) (Gallistel and Leon, 1991; Leon and Gallistel, 1998; Simmons and Gallistel, 1994). In the case where the behavioral responses saturate with an increase in current used in combination with stimulation frequencies well within the range of the physiological responses of reward relevant axons, there seems to be a limit on the maximum reward value the integrator can represent (Gallistel et al., 1991; Simmons and Gallistel, 1994). At some point, regardless of how many more action potentials are generated by the reward cable, the output of the integrator is limited. Therefore, it is thought that there is a ceiling to the amount of reward a rat can experience. Conversely, there can be a ceiling on the inputs to the integrator. Electrophysiology experiments have shown that stimulation

frequencies greater than 250Hz cannot be followed by the reward axons stimulated by BSR (Forgie and Shizgal, 1993). Knowing stimulation parameters that provide either saturated input to the integrator or cause the integrator's output to reach a ceiling are potentially useful tools for identifying the neural basis of a putative reward integrator.

Anatomical Substrates

One of the most striking effects of electrically stimulating the medial forebrain bundle is how vigorously it fuels subsequent behavior aimed at acquiring additional stimulation. We have previously mentioned evidence linking this rewarding effect to those produced by natural stimuli such as sucrose and by drugs of abuse. Still, identifying the neural substrate responsible for the rewarding effects of MFB stimulation has proven difficult, in large part due to the anatomical complexity of the regions being stimulated. Anatomical studies of the MFB reveal that it is comprised of up to 50 different types of projections and involves some 13 different neurotransmitters (Nieuwenhuys, Geeraedts et al. 1982). The MFB is a diffuse fiber system that contains ascending and descending projections with both myelinated and umyelinated axons. It has a substantial projection from forebrain areas including the olfactory tubercle, septum, lateral preoptic area that descend onto cells in the tegmentum. This projection primarily consists of myelinated axons. There is also a very prominent ascending projection consisting of unmyelinated axons with somata in VTA. These axons can release dopamine, GABA, glutamate, and possibly other neurotransmitters.

The structure most often stimulated to produce BSR effects is the medial forebrain bundle (MFB) at the level of the lateral hypothalamus (LH). The MFB is a complex bundle of both ascending and descending axons that extends from basal

olfactory regions through the lateral hypothalamus caudally to the ventromedial part of the tegmentum mesencephali (Figure 2) (Nieuwenhuys et al., 1982). Although other sites outside of the MFB including prefrontal cortex, cerebellum, hippocampus and locus coeruleus can also sustain self-stimulation (Shizgal, 1997), the MFB is the preferred site because it most robustly supports self-stimulation. Animals stimulated in the MFB have high response rates and exhibit excited and agitated behavior. A great deal of effort has gone into identifying the neurons directly stimulated by electrodes implanted in the MFB and their targets. Several electrophysiological studies have concluded that the directly stimulated fibers responsible for BSR have fine and myelinated axons (Gallistel, Shizgal et al. 1981; Yeomans 1989). These axons have somata located rostral to the MFB with synaptic targets in the ventral tegmental area. This is not consistent with the direct stimulation of dopaminergic fibers which have unmyelinated, slow conducting axons (Murray and Shizgal 1996). This finding has generated a hypothesis referred to as the "descending path hypothesis" (Bielajew and Shizgal 1986).

Other groups aiming to elucidate the origins and targets of the reward relevant neurons have challenged the idea of the "descending path hypothesis" based on lesion studies. Lesions rostral to the MFB electrode in conjunction with 2-deoxy-glucose (2DG) measurements were made to test the functional connectivity between the basal forebrain and VTA. These studies show evidence that specific forebrain nuclei remain structurally and functionally connected to the midbrain after MFB lesions, and they surmise that the descending path hypothesis is not complete; there may well be other fiber pathways involved as well (Gallistel, Leon et al. 1996; Simmons, Ackermann et al. 1998).

The role dopaminergic neurons play in BSR is still contested. Several studies investigating the neurophysiological properties of dopamine neurons conclude that the refractory periods of DA neurons are too long, and their conduction velocities are too slow for them to support the stimuli used in BSR (Bielajew et al., 1982; Bielajew and Shizgal, 1982). There is a substantial amount of evidence showing that dopaminergic neurons are activated trans-synaptically by rewarding brain stimulation (Moisan and Rompre, 1998). It is clear that techniques which provide a larger view of the anatomy are necessary to better understand the structure of the neural substrate responsible for reward.

A major target of the ascending umyelinated axons coursing through the MFB is to the ipsilateral nucleus accumbens (NAc). The projection from VTA to the NAc has the highest proportion of dopamine afferents, approximately 65% - 85% dopaminergic. It has also been shown that VTA has other projections that are comprised of dopamine in varying degrees: the lateral septal area (72%), amygdala (53%), entorhinal cortex (46%), PFC (30%–40%), and hippocampus (6%–18%) (Fields, Hjelmstad et al. 2007). What functional role does such a rich dopaminergic projection serve in the NAc is a topic of substantial research. Several groups have shown that the release of dopamine can both excitatory and inhibitory (Nicola and Malenka 1997; Nicola, Surmeier et al. 2000; Brady and O'Donnell 2004; Kita, Parker et al. 2007). Dopamine release can have such varying effects on postsynaptic targets via two families of dopamine receptor types. The D1-like family of receptors consists of D1 and D5 receptors, and the D2-like family is composed of D2, D3, and D4 receptors. Both families are G-protein coupled receptors, and they exert their effects by activating G-proteins which catalyze inhibitory

or excitatory signal transduction pathways (Nicola, Surmeier et al. 2000). Therefore, similar to other G-protein coupled transmitter systems, dopamine functions as a modulator of other incoming excitatory input that serve as the drivers of activity in the NAc.

Virtually all the major neurotransmitters in the brain play some role in reward. A brain area that has repeatedly been shown to be involved in reward related behaviors is nucleus accumbens (NAc). The NAc is primarily composed (95% of neurons) of medium spiny GABA-ergic neurons (Chang, Wilson et al. 1982), and it is thought to have a special role in reward processing because it receives input from both limbic and motor areas (O'Donnell, Greene et al. 1999). Studies have shown that glutamatergic excitatory afferents converge onto NAc neurons from the hippocampus, amygdala, and prefrontal cortex (Pennartz, Groenewegen et al. 1994; Floresco, Blaha et al. 2001). Furthermore, anatomical tracer experiments demonstrate that a GABA-ergic as well as a very rich dopaminergic projection originates from neurons in the VTA and synapse onto medium spiny neurons in the NAc (Fallon and Moore 1978; Sesack and Pickel 1990). As such, the nucleus accumbens has been implicated in various motivational, behavioral, and cognitive functions including instrumental learning, novel stimuli salience, and locomotor activity (Delfs, Schreiber et al. 1990; Cousins, Sokolowski et al. 1993; Berns, Cohen et al. 1997).

Role of functional MRI for studying rodent behavior

The fMRI methods we are using will allow us to follow brain activity patterns noninvasively at modest spatial resolution (hundreds of microns) and with temporal resolution in the order of seconds (Jezzard, Matthews et al. 2001). As in other fMRI

applications, brain activity is recorded indirectly, via changes in blood oxygenation, volume and flow also referred to as the blood oxygenation level-dependent (BOLD) effect (Ogawa, Lee et al. 1990). BOLD is a useful tool for mapping of neural population dynamics, and for the studies performed here it offers the important advantage of whole brain coverage. fMRI is most commonly used to relate signal changes in each volume element (a voxel) to a specific stimulus. Activation maps are generated by considering which voxels are correlated with stimulus presentation at an appropriate significance level.

More traditional methods for activity mapping in small animals are 2-deoxyglucose (2DG) autoradiography and immediate-early gene (IEG) histochemistry (Sokoloff, Reivich et al. 1977; Sharp, Sagar et al. 1993; Guzowski, Timlin et al. 2005). In 2DG methods, a radioactive glucose analog is used to label cells in proportion to their metabolic activity levels. Animals are sacrificed after a 2DG labeling period during which animals perform a task or undergo stimulation (Esposito, Porrino et al. 1984; Porrino, Esposito et al. 1984). 2DG distribution is determined by autoradiography of sectioned brains and areas of differential activation are identified by comparing between test and control groups. The IEG method relies on the induction of certain genes by increased neural activity, as part of the process by which synaptic plasticity takes place. IEG induction is measured after sacrifice and brain sectioning by in situ hybridization with probes for IEG transcripts, or by detecting IEG proteins. IEG mapping is often preferred to the 2DG method because it has true cellular resolution (Sharp, Sagar et al. 1993; Guzowski, Timlin et al. 2005); although, IEG upregulation is not as tightly coupled to neural activity as 2DG uptake. Compared with either of these methods, fMRI techniques

offer specific advantages: (1) in our experiments we can vary the intensity of a rewarding stimulus and look for systematic changes in the BOLD response. (2) experiments can be performed on the same animal across multiple sessions. (3) fMRI results can be used to guide invasive experimental techniques. In combination, these advantages allow fMRI to yield much more precise information about what conditions influence the activity of neural populations, despite having considerably lower spatial resolution than either 2DG or IEG.

Summary

A working model of the role of reward in decision making has slowly emerged from the work described above, and is depicted in Figure 1. A wide array of naturally occurring stimuli are known to be rewarding, including sexual pheromones, water, gustatory cues, such as sodium, sugar, etc. Each of these are represented via distinct processing pathways, and are modulated by internal states and learned associations related to each modality. Signals along these pathways are ultimately converted to a common reward currency. It is this transformation to a common currency which allows comparisons of rewards of different modalities. Artificial rewards, such as BSR and potentially some drugs of abuse interact with the system at this level. The common reward signal is summated to generate a representation of the value of reward received. It is at this stage that prediction error is calculated between the received reward, and the expected reward. A large body of work has suggested that this prediction error signal is represented by the activity levels of midbrain dopamine neurons in the VTA and SNR (Schultz, Dayan et al. 1997; Bayer and Glimcher 2005; Pessiglione, Seymour et al. 2006). Finally, the value of the reward magnitude is accessed by decision-making

circuits, which compute a probability of choice, according to Herrnstein's matching law. An action is then chosen from this probability distribution. Our studies focus on elucidating the processes responsible for computing and representing reward magnitude. We use BSR to access the neural circuitry which transforms sensory inputs into a common reward currency, and by manipulating the frequency of stimulation of the BSR delivered, we can isolate brain regions that follow a psychometric response function which we know from Herrnstein's Law to be a direct measure of subjective reward magnitude.

Specific Aims

The goal of this thesis is to elucidate the neural circuitry underlying reward integration and reward magnitude representation. Specifically, our aim is to identify neuronal populations in the brain that encode reward values. Our approach is to use a multidisciplinary approach, combining rewarding electrical brain stimulation, psychometric assessment of reward magnitude, fMRI measurement of whole brain activity, and visualized focal inactivation of specific neural structures.

We first measured the subjective reward magnitude in behaving rats using established behavioral paradigms and quantitative psychometric measurements. Subsequently, in the same rats, we attempted to strip away all of the complexities of the awake behaving context and isolate the most elementary, first-order reward value representation. We repeated the identical electrical stimulation protocol in the same animals, under anesthesia, while measuring neural activity with BOLD fMRI. Thus, the representation that we aimed to elucidate is equivalent to the representation of the common reward currency (see Figure 1); it is independent of the context and modality-

specific cues that would naturally activate it, and of the decision-making circuits that would access it.

Identifying neural elements activated by rewarding electrical brain stimulation of the medial forebrain bundle

Our first aim was to identify brain areas that are activated by BSR. Functional MRI experiments were performed on anesthetized rats receiving rewarding electrical brain stimulation to characterize brain regions that respond differentially to varying degrees of rewarding electrical brain stimulation intensity. fMRI data were obtained from rats implanted with medial forebrain bundle electrodes and that had previously been trained to discriminate between stimuli varying in intensity of reward. These experiments provide a framework of brain areas potentially involved in the representation of reward magnitude.

Identifying structures that represent reward magnitude

Our next aim was to isolate neural populations that directly represent reward value, and distinguish them from other activated areas that may play different roles in reward processing. We measured psychometric reward value curves in behaving rats, and subsequently imaged the activity due to the identical stimulus frequencies presented during the behavioral task. We then analyzed the responses to identify brain structures that specifically tracked the behavioral reward curves. This analysis provides a whole-brain view of the distributed network of brain regions that represent subjective reward magnitude.

Determining the role of the ventral tegmental area in the reward magnitude representation

Our last aim was to test the role of descending fibers that terminate in VTA on the whole brain reward representation. If the descending pathway hypothesis is correct, inactivating VTA should have wide-ranging effects on rostral brain activation. Based on our descriptive analysis of the reward representation, inactivation of VTA should alter both the reward curve measured behaviorally, and the neural activity in downstream brain regions. We investigated this idea using site-specific pharmacological inactivation, in combination with MFB stimulation and fMRI. This experiment allows us to go beyond the descriptive analysis, and specifically assign the nature of the role of these brain regions in the representation.

Methods

Implantation of stimulation electrodes

Adult male Lewis rats (150-300 g) were implanted with stimulation electrodes in the MFB at the level of the lateral hypothalamus, using stereotaxic coordinates. Monopolar electrodes were fabricated with teflon-coated silver wire, 0.063 mm diameter, cut to a length of approximately one centimeter. The electrode tip was formed by the cut end of the wire, with additional stripping. Wire was threaded through polyimide tubing for mechanical support and connected to a 2-pin interface. One pin was attached to the electrode wire using silver paint, and the second pin was attached to a stripped reference wire made of 0.125 mm diameter silver. Prior to surgery, each animal was anesthetized with 1% isoflurane and positioned on a stereotaxic device (Kopf). An incision was made along the midline of the skull, and the scalp was retracted to expose a one centimeter width including the implantation site. A microdrill (Fine Science Tools) was used to introduce a hole in the skull 2.0 mm posterior to bregma and 1.7 mm left of the midline suture. The electrode tip was lowered through this hole, to a depth of 8.6 mm below the skull surface at the level of the lateral hypothalamus. An additional hole was drilled through the skull approximately above the cerebellum for introduction of a conducting, MRI-compatible screw (BeCu; Antrin Enterprises); the electrode reference wire was wound around this screw and attached with silver paint. One other shallow hole for a nonconducting skull screw was drilled over the contralateral cerebellum. Animals implanted with a 7.5 mm long guide cannula (Plastics One, Inc) for the infusion of lidocaine into VTA (-5.2 posterior to bregma, 0.9 mm lateral to bregma, 7.5 mm below the skull) had the stimulating electrode implanted in a slighted

altered located in order to accommodate both the electrode and guide cannula into the window of the imaging surface coil. These animals had a stimulating electrode implanted into the lateral hypothalamus at slightly more anterior location (-1.2 posterior to bregma, 1.7 mm lateral, 8.7 below the skull surface). Dental cement was applied to the entire skull surface area to hold the electrode rigidly in place. The animal was allowed to recover from anesthesia under supervision. Buprenorphin (0.03 mg/kg) was injected subcutaneously before surgery and twice daily for the two-day period following. Electrode positions were confirmed using MRI data. All surgical and animal handling procedures were approved by the MIT Committee on Animal Care.

Preparation for imaging anesthetized animals

Prior to imaging, rats which had been subjected to the behavioral shaping were anesthetized with 3% isoflurane and tracheotomized. Each animal's neck was shaved and an incision made roughly from the chin to the rib cage. Skin and muscle were retracted and the trachea exposed. The trachea was opened with surgical scissors and a luer-fitted teflon cannula (McMaster-Carr) was inserted, with the tip oriented towards the lungs. The cannula was fixed in place using dental floss. Then the wound was closed with biocompatible glue (Vetbond, 3M). Tracheotomized animals were paralyzed with 1 mg/kg intraperitoneal pancuronium and mechanically ventilated using an Inspira ventilator from Harvard Apparatus, operated at 70 beats per minute and 5 mL per stroke. Heartbeat and blood oxygenation were continuously monitored using a noninvasive infrared sensor and pulse oximeter (Nonin Instruments). Animals were wrapped in a heated circulating water blanket (Gaymar). They were then transferred to a plastic positioning device (Ekam Imaging) for imaging and placed into a 4.7-T Bruker

Avance scanner. We monitored heart rate continuously during the delivery of BSR using a Nonin Medical 8600V pulse oximeter equipped with a nonmagnetic sensor. The stimulating electrode was connected to a stimulator located outside of the scanner. These animals were maintained on 1% isoflurane and 1 mg/kg/hr pancuronium for the duration of the scanning session.

Histology

After imaging or behavioral session involving lidocaine inactivation, we placed rats under terminal anesthesia with ketamine and xylazine and transcardially perfused them with phosphate buffer containing heparin (Hospira) and then with 4% paraformaldehyde (Electron Microscopy Sciences). We removed brains and obtained coronal sections of 50 µm or 100 µm thickness at across a range extending ~1 mm anterior and posterior to the injection cannula insertion site. Sections were Nissl stained to visualize the position of the electrode and infusion cannula relative to the boundaries of brain structures.

Behavioral and stimulation apparatus

All behavioral experiments were performed in a plexiglass operant chamber (28 x 21 x 21 cm L x W x H; Lafayette Instruments), placed in a lighted sound-proof cabinet (Med Associates). Two infrared nosepoke sensors (Med Associates) were positioned at one end of the chamber; 5 cm from the floor, and a light emitting diode (LED) was positioned near the top of the chamber above the sensors. Input from the nosepoke sensors was monitored by a Macintosh G3 laptop computer via a digital input/output interface (National Instruments). A computer program was developed in C (Metrowerks

Codewarrior) to time output stimuli dependent on the detected nosepokes. Output pulses (5 ms) from the computer were used to trigger shorter cathodal stimulus pulses (0.1-0.5 ms) delivered by a constant current isolated stimulator (World Precision Instruments, Inc.). Poles of the stimulator were shorted to one another in between stimulus pulses to prevent charge buildup on the electrodes, and pulses were visualized on an oscilloscope to verify rectangular pulse shape.

Behavioral shaping

Behavioral experiments proceeded in several stages: In the first stage, electrode-implanted rats were connected to the stimulator and released into the operant chamber for unsupervised training (shaping). In a typical experiment, an animal would be rewarded for each nosepoke with a one second 150 Hz sequence of 0.2 ms pulses, at the maximum stimulus current (typically about 0.7 mA) at which no stimulus induced motion was observed for 150 Hz stimulus frequency, and with a minimum interstimulus spacing of 0.5 seconds. Shaping sessions lasted 30 minutes to one hour, once per day; animals which failed to perform vigorous operant responding for brain stimulation where considered for the high-frequency group (reference frequency of 300Hz). For preliminary data presented here, animals subjected to training on a two-choice test were imaged.

Reward titration curve measurement

Two-choice tests were used to determine reward titration curves and the threshold for reward saturation; these curves provide a quantitative behavioral measure of BSR value, for correlation with fMRI results. The titration procedure was based on studies of Gallistel, Shizgal and others, who have shown that rats prefer rewards of

increasing intensity (here BSR frequency) up to a saturation threshold beyond which more intense stimulation is indistinguishable from the saturation threshold reward. In the two-choice test we used to measure this phenomenon, a fixed current (maximized without producing movement), pulsewidth (0.2 ms), train length (1 s), and minimum intertrain interval (0.5 s), were applied with variable stimulation frequencies in order to produce stimuli of varying intensities. Each of the two nosepokes was associated by the computer program with a particular reward intensity/frequency. Within a given session, one of the frequencies was fixed (the "reference" frequency) and the other was varied over a factor of 1.2, evenly spaced in log units around the reference (the "comparison" frequency). Training sessions consisted of 10 five-minute trials (with 30 s intertrial intervals) in which different comparison stimuli were offered to the animal in parallel to the reference frequency. One of the two nosepoke holes was randomly associated with the reference frequency at the beginning of each trial, and the other was associated with the comparison frequency; halfway through each trial, the correspondence was switched. Nosepokes at each hole were automatically rewarded by the operant scheduling program, and both input and output events were recorded.

Magnetic Resonance Imaging

A single-shot gradient echo planar imaging (EPI) sequence was used for standard BOLD imaging in a 4.7T magnet. Image matrices of 64 x 48 pixels were acquired using TE/TR 20/2000 ms, field of view 3.2 x 2.4 cm and slice thickness of 1mm. Imaging volumes consisted of 14-16 consecutive slices centered over the somatosensory cortex. High resolution anatomical images of the forebrain, including

electrode implantation site, were acquired using a gradient echo FLASH sequence (TE/TR 15/2000 ms, 256 x 256 matrix, 3 x 3 cm FOV, slice thickness 1mm).

We acquired fast spin echo (FSE) MRI scans (TE/TR 14/277 ms, 8.9 s per scan, 0.3 × 0.3 × 1.0 mm resolution, 3.8 × 3.8 cm FOV, data matrix 128 × 128) before infusion of the lidocaine/Gadolinium-DTPA (a complex of gadolinium with a chelating agent) mixture and continuously during the bolus infusion (10 min) of the solution. Gd-DTPA is a non-toxic T1 contrast agent that allows for the visualization of the lidocaine injection *in vivo*. Lidocaine mixed with Gd-DTPA (1mM) was injected for 10 minutes at rate of 0.1 µl /min prior to the commencement of the delivery of electrical brain stimulation. The infusion of the lidocaine mixture was maintained at the same rate throughout the entire BOLD imaging session during which BSR was administered.

Diffusion Tensor Imaging

Diffusion Tensor Imaging (DTI) provides information about fiber tracks in the brain. Diffusion of water in the direction of the fibers is faster than in the perpendicular direction. This feature allows experimenters to map out the orientation in space of the white matter tracks in the brain using a color scale. Structural information of white matter connectivity is used to align brain images across rats in addition to aiding localizing regions of interest for BOLD fMRI data analysis.

Data Analysis

MRI data were processed using custom routines running in Matlab (Mathworks). Data from all experiments was Fourier transformed with a spatial smoothing kernel of one voxel half-width. Activation maps (spatial distribution of voxels with signal intensity significantly correlated with the stimulus, usually color-coded by correlation coefficient)

were calculated using the AFNI software package (NIMH, Bethesda, MD). A least squares volume registration algorithm running in AFNI was used for motion correction of data, after masking out signal from outside the brain. Affine registration of data from multiple animals, and alignment of functional maps with anatomical images was performed using a landmark based least-squares fitting procedure implemented in AFNI. Further processing, including extraction of region of interest (ROI) timecourses, data averaging over stimulus cycles, and correlation with behavioral data was performed in Matlab.

Differentiating Activity from Large Draining Veins

Because fMRI relies on changes in blood oxygenation as a means of inferring neural activity, a potential contaminant in BOLD fMRI studies originates from signals in macrovasculature, or large draining blood vessels. The most relevant cortical activity detected with BOLD signals is within the microvasculature of gray matter; large draining veins can produce changes in BOLD that are not co-localized to voxels with active parenchyma. As a result, contributions of signal from the draining veins will result in a loss of spatial resolution of the assignment of neural activity. Efforts must therefore be made to minimize these contributions. One means to accomplish this is to take advantage of the different time-courses of activation in micro- and macro-vasculature. The BOLD signals in the large draining veins are delayed by several seconds relative to the signals in cortical tissue. Changes in BOLD response in gray matter are delayed 4 – 8s from the onset of a stimulus, whereas signals in large vessels are shown to be delayed by 8 – 14s (Lee, Glover et al. 1995). Taking this fact into account, we adapted

methods for excluding voxels with large vessel contamination to our stimulation protocol (Menon 2002; Kim and Ugurbil 2003). We computed the response maps from the last two of the eight stimulus trains in each cycle (Figure 4a). Due to the delay of the BOLD effect in large draining vessels, these responses should contain a relatively large contribution from them. We then calculated the same maps from the first two trains in each cycle (Figure 4b). The difference between these maps (Figure 4c) was used to create a mask of the voxels with a high contribution from large vessels (Figure 4d). By visual inspection, we confirmed that the overall shape of the mask bore a strong relationship to the location of large veins (Paxinos 2004). This mask was subsequently applied to all the functional maps, in order to ensure that our BOLD measurements were dominated by micro-vascular gray matter activation. We confirmed the effectiveness of this procedure by comparing the time-course of the BOLD changes averaged over one cycle of stimulation for voxels within the mask, and for an example ROI, the pre-optic area (PO) (Figure 4e). We chose this area for comparison, because it is located in close proximity to a large vein which was included in our mask. The large draining component is clearly visible in the time-course of the response as a gradual rise in the signal which is underlying the short-latency responses to each individual train of the stimulus (the "spikes" in the graph). By contrast, the time-course in PO is dominated by the short-latency individual responses. This comparison provides strong evidence that our post-acquisition analysis procedure effectively removed the voxels with substantial large vessel contamination.

RESULTS (CHAPTER 2)

Our first goal was to map the brain regions that are activated by rewarding electrical brain stimulation (BSR) of the lateral hypothalamus. Rats were chronically implanted with stimulating electrodes in the lateral hypothalamus and were trained in a two-choice operant task. Rats which performed the task at a high level of responding were included in the fMRI phase of the experiment. In the second phase, rats were anaesthetized and received identical electrical stimulation trains while being imaged in a 4.7T magnet. BOLD (blood oxygen level dependent) signal changes were recorded as a metabolic surrogate of neuronal activity. The spatial patterns of increases in BOLD activity were used to map out the brain regions activated by the stimulation.

Global activation patterns resulting from rewarding brain stimulation

A group of ten rats was imaged in this way, and combined in a group analysis. Figure 3 shows the activity patterns resulting from BSR. We observed a distributed pattern of activation throughout nearly the entire rostro-caudal extent of the brain. Statistically significant activation occurs in a large portion of the brain (56% of voxels). This is likely due to the widespread projections that course through the MFB. Particularly strong "hotspots" of activation are seen in several regions, including the ipsilateral ventral striatum and hypothalamus, contralateral thalamus and bilateral midbrain. Several of these areas have been previously implicated in reward processing. In order to specifically determine the anatomical brain areas that are highly activated, we performed a region-of-interest (ROI) analysis. Using landmarks from co-registered

diffusion tensor imaging (DTI) and anatomical images, we assigned ROIs to brain regions defined by Paxinos and Watson (Figure 5). We then computed the amplitude of the BOLD response in each of these brain regions. The most strongly activated areas include the preoptic area, olfactory tubercle, lateral hypothalamus, substiantia nigra (SN), and ventral tegmental area (VTA) (Figure 6a).

This analysis provides an overall picture of the brain regions that are activated by the BSR. There is extensive overlap between the regions that we have identified as most strongly activated, and those that have been identified using other methods, including 2-DG and c-*fos* staining (Gallistel, Karreman et al. 1977; Arvanitogiannis, Flores et al. 1996).

Reward magnitude tracking

In and of itself, the preceding analysis does not directly identify the brain structures involved in the computation and representation of reward magnitude *per se*. For example, a number of projections through the lateral hypothalamus are unrelated to reward but nonetheless are likely directly activated by the electrical stimulation (Shizgal, Bielajew et al. 1980). Additionally, there are a number of reasons why the amplitude of BOLD activity is not a direct measure of the importance of a structure to reward processing. For instance, mono-synaptically activated neural populations might inherently exhibit larger BOLD responses, which may disguise the true importance in reward processing that may take place in structures that are activated through poly-synaptic connections.

With these considerations in mind, we sought to disambiguate brain regions with direct roles in processing of reward magnitude from areas simply directly stimulated by

the electrical stimulation. To do this, we made use of a behavioral paradigm that has been shown to directly measure reward magnitude. This paradigm relies on Herrnstein's matching law, which describes how animals distribute their choices based on the magnitude of reward received at the available options. The matching law states that animals will allocate behavioral response rates in direct proportion to the rate of reward received at a particular option.

Behavioral frequency-response analysis

In this study rats were presented with a two-choice operant task where the two choices (nose-pokes) trigger the delivery of a different magnitude of BSR. During each trial, one of the nose-pokes delivers a fixed frequency of rewarding stimulation (the reference; 150Hz), and the other nose-poke delivers a pseudo-randomly selected comparison frequency of stimulation (Figure 7a). This task enables us to quantitatively assess how rewarding each comparison frequency is perceived to be by measuring the number of times it is chosen relative to the reference frequency. For example, if the comparison frequency were equal in reward magnitude to the reference frequency, the number of choices allocated to each nose-poke would be the same. By computing the relative response rates to ten comparison frequencies, we are able to generate a psychometric reward magnitude curve. As can be seen in Figure 7b, the subjective reward magnitude does not scale linearly with the frequency of stimulation. This saturating frequency-response curve has been observed under similar conditions by several other groups, starting with Gallistel (Simmons and Gallistel 1994). Using this unique psychometric response curve, we are able to better identify brain structures that are directly involved in representing reward magnitude.

Neural frequency-response analysis

Our approach is to identify neural populations that exhibit a similar neural response profile to that seen in the behavioral curve, and therefore tease out the reward circuit from non-reward related areas incidentally activated by the stimulation. Performance of the task by the awake rat requires several brain circuits to work in unison. In addition to the reward circuit itself, other factors such as motivational state, memory recall, and action circuits are likely to be engaged. Our goal is to strip away the influence of these other factors in order to isolate the mechanism through which the brain is able to construct a representation of reward magnitude in order to guide behavioral choices.

In an MRI scanner, we deliver the same frequencies of electrical stimulation presented during the behavioral task in a block design (Figure 8a) while recording BOLD responses from the entire brain. Figure 8a depicts our experimental design. The top panel shows the timecourse of responses to the pseudo randomly presented BSR from the lateral hypothalamus. Figure 8b shows the response in LH to one cycle of BSR, where one cycle consists of eight one-second pulse trains. Figure 8c shows the average response to each frequency sorted in ascending frequency order. From these responses we then compute a frequency response curve for each voxel.

In order to identify brain structures involved in reward magnitude representation, we first computed the average frequency-response curves for each ROI. Figure 9b shows examples from two brain areas, VTA and the NAcs. The responses in the VTA increased linearly across the entire range of stimulation frequencies tested. The NAcs showed pronounced saturation of response as frequency increased above a threshold.

Thus, visual inspection of the curves suggests that some brain regions indeed track the subjective reward magnitude. In order to confirm this observation, we developed a quantitative model to differentiate linear from behavior-tracking curves.

Frequency vs. behavioral models

We then used a general linear model to test the contribution of these two potential factors to the BOLD frequency-response curves. For this model, we made the assumption that at the level of neural populations, activity evoked by the stimulation, but unrelated to reward magnitude tracking would correspond to the frequency of stimulation in a linear fashion. In contrast, activity related to the computation or representation of reward magnitude would have a frequency-response profile that is similar to the psychometric behavioral function. Our model therefore incorporated two factors, a linear regressor, and a regressor that was an idealized version of the average behavioral curve of the imaged rats (Figure 9a). We ran a regression to fit the curve from each brain region, and compared the coefficient weights and statistical contribution to the fit. The results of the regression are color coded such that red denotes that the activity is best modeled by the behavioral regressor, green indicates that the linear model best fits the activity, and yellow indicates that both factors contribute significantly. These two examples demonstrate the first two possible outcomes of this analysis; the curve for the NAcs is red, demonstrating that only the behavioral regressor made a significant contribution ($p<0.05$, Bonferroni corrected) to the model fit to the curve and the curve for the VTA is green, demonstrating that only the linear regressor made a significant contribution to the model fit to the curve.

Using the model, we tested the contribution of these two factors at each voxel in the brain, to generate maps which identify whether the response from a voxel is modeled by either regressor in a statistically significant way (Figure 9c). This analysis makes apparent that the majority of the significantly activated voxels linearly track the stimulation frequency. This suggests that these areas likely do not contribute to the computation or representation of the reward magnitude elicited by stimulation, per se. The minority of voxels that appear red in the maps are of particular interest, because they are likely to be directly related to reward magnitude. The reward tracking regions are largely concentrated in a few particular brain structures: the ipsilateral nucleus accumbens and amygdala, and the contralateral thalamus and caudate-putamen.

To more specifically address the brain regions involved in reward magnitude processing, we performed the same analysis of the frequency-response curves at the ROI level. In Figure 10, we show the average curves for each ROI, color-coded according to the same color-code as in Figure 9, with red corresponding to significant contribution from the behavioral regressor, green significant for the linear, yellow significant contribution from both factors, and gray neither. The only area that is significantly modeled by the behavioral factor under this criterion is the NAcs. This suggests that the NAcs is the primary site of reward magnitude representation in the brain.

However, it is apparent from Figure 9c that there are distinct clusters of voxels within other brain regions (for instance the amygdala) that have a significant contribution from the behavioral regressor. We made the ROIs based solely on the anatomical boundaries specified by the Paxinos et al atlas (Paxinos and Watson 2007). However,

many brain structures are known to have functional subdivisions within them, many of which are too small to be confidently labeled on the basis of our ROI assignment procedure alone. In fact, apparent functional segregation within some ROIs can be seen in the maps generated by the voxel-wise regression. Furthermore, at the neural level there may well be heterogeneity of frequency-response profiles within a brain structure, even in the absence of visually apparent spatial clustering. The activity of such a neural subpopulation would be obscured by averaging the all the voxels within an ROI.

To address this possibility, we devised the following analysis. Within each ROI, we tested whether there was a bi-modal or uni-modal distribution of voxels using Hartingan's dip statistic (Hartigan 1985). In many cases, there were ROIs that had bi-modal distribution of linear and saturating voxels (Figure 11). We isolated the 33 percent of voxels with the largest beta weights for the linear and behavior-tracking regressors, and analyzed their frequency-response curves independently. We modeled the contributions of the two regressors as before to the average curves from these subsets of voxels. Our goal was to determine for each brain region whether some subset of neural activity could plausibly be involved in the reward magnitude representation. As seen in Figure 12, for many brain regions, even the most behavior-tracking voxels have a significant contribution from the linear regressor (e.g. the hippocampus). However, a number of regions contain a clearly behavior-tracking subset of voxels. Figure 13 shows the curves computed from the top 33% most saturating and the top 33% most linear voxels in two such ROIs, the NAcc and the AmygAM. The clearly saturating portions of these ROIs suggest that sub-populations of those brain areas are involved in the representation of reward magnitude.

Behavior-tracking not explained by saturation of neuro-vascular coupling

Since we are relying on BOLD activity as a surrogate for neural activity, one potential confound is saturation of the neuro-vascular coupling mechanism – ie, that the BOLD signal can no longer increase as the neural response continues to increase. If that were the case, then the saturation of the frequency-response curve, which we are attributing to the reward magnitude representation would be an artifact. To examine this possibility, we performed a number of analyses. If BOLD saturation were responsible for saturation of the curves, we would expect saturation to be most prominent in voxels with the largest BOLD response magnitude. When we plotted the maximum BOLD response (for any stimulus frequency) against the beta weight of the significant linear and behavior regressor for each voxel (Figure 14), we saw the opposite trend. The significantly linear voxels tended to have larger BOLD responses. This analysis assumes that the transformation of neural activity to BOLD is uniform across all voxels. To avoid depending on this assumption, and to be sure that BOLD saturation is not confounding our interpretation, we independently compared the magnitude of BOLD with the degree of reward curve saturation. To do this, we computed the average maximal BOLD response across all voxels in each ROI which were significantly saturated, significantly linear, both or neither. Across the all ROIs, we again found the same trend apparent in Figure 14; the most saturated voxels tended to have lower response magnitude than the more linear voxels (Figure 15a). Within individual ROIs, there was higher variability in this relationship (Figure 15b). However, there was not an apparent bias towards larger BOLD in the more saturated voxels within the ROIs which

we have concluded to have reward saturation (the NAc and the amygdala). These analyses, demonstrating that even the most strongly responsive voxels do not necessarily saturate, strongly argues that neurovascular-coupling is not the source of saturation in the frequency response curves.

High frequency analysis

The MFB is a complex fiber bundle, containing a large variety of axons with cell-bodies of origin ranging across nearly the entire brain. Not all of the axons coursing through the MFB are related to reward. However, electrical stimulation does not readily discriminate among these fibers. It is therefore likely that some of the activation that we observe is not related to reward in any way. This topic has received considerable attention in the literature, and a number of efforts have been made to distinguish the reward-relevant axons based on their biophysical properties (Gallistel, Shizgal et al. 1981; Yeomans 1989). In fact, the stimulation parameters that we have used in the preceding experiments, were based on this literature, and were carefully chosen to maximize the recruitment of the reward-relevant fibers. We next exploited this knowledge to further tease apart the reward-relevant from reward-*irrelevant* activation.

As described in the section on the "counter model" (see Background), the perceived subjective reward resulting from BSR is thought to be determined by a trade-off between the number of reward relevant fibers stimulated, and the number of impulses carried by each fiber within a certain integration window. As such, the reward pathway should be subject to certain biophysical constraints. There is a limit to the number of fibers that can be recruited by a stimulating electrode. There is also a limit to the frequency-following capacity of the reward-relevant fibers themselves. Using a

behavioral readout, careful biophysical studies, using collision tests and refractory period analysis to determine the frequency-following limits of the relevant fibers have demonstrated that the reward-relevant fibers are unable to faithfully follow frequencies above ~250Hz (Forgie and Shizgal 1993). This is not to say that other fibers within the MFB cannot follow higher frequencies. We made use of this information to constrain the brain regions that may be responsible for the representation of reward magnitude.

We trained a second group of rats using a different stimulation regime: lower currents in combination with higher frequencies. The stimulation frequencies in this case extended well above the frequency-following cutoff of the reward-carrying fibers. As in the low-frequency regime, we were able to generate psychometric frequency-response curves which exhibited a sigmoidal shape (Figure 16a). Note that the fact that the curves continue to increase above the saturation frequency from the low-frequency regime (~130Hz) adds additional evidence that the saturation in the low-frequency regime was not due to an artifact from neural frequency-following or saturation of neuro-vascular coupling.

We then analyzed the BOLD responses as a function of stimulation frequency in these rats, using the same analysis methods used for the low frequency data (Figure 9c). Figure 16b shows the results of the linear vs. behavior regression obtained from these data. Based on previous work described above, we assume that reward-relevant axons do not increase their activity substantially above 250Hz. Thus, activity which saturates at, or below, 250Hz has an ambiguous interpretation. The saturation may result from the reward integration mechanism, or from the inability of stimulated axons to follow the stimulation frequency. We can conclude that saturated brain regions could

plausibly be involved in reward magnitude representation. Conversely, activity that increases linearly above 250Hz may be unrelated to reward processing of the BSR. We observe that the contralateral thalamus, and the bilateral cingulate cortex are better described by the linear model. This suggests that these regions are *not* directly involved in the rewarding aspects of BSR. This additional test, in combination with our previous analyses will help us narrow down the network of brain structures that are involved in the representation of reward magnitude.

Influence of VTA on network activity

The analysis to this point has suggested a network of brain regions which are involved in the computation and/or representation of subjective reward magnitude. Both NAc and Amyg receive substantial input from VTA, the structure most commonly associated with reward processing in mammals. An array of circumstantial evidence points to a key role for VTA in reward processing. One particularly influential hypothesis has been put forward for the circuit underlying the rewarding effects of BSR. In this model, the directly stimulated reward-relevant fibers are the myelinated axons originating in the basal forebrain, and descending to synapse on the dopaminergic neurons in the VTA (Bielajew and Shizgal 1986; Yeomans 1989). Trans-synaptically activated dopaminergic neurons subsequently project rostrally, and mediate the rewarding effects on target areas such as the nucleus accumbens. This model was proposed as an attempt to reconcile two observations: a) the reward relevant axons are descending, and have refractory periods inconsistent with the biophysical properties of the axons of dopaminergic fibers originating in the VTA (Bielajew and Shizgal 1986; Yeomans 1989), and b) dopamine appears to be involved in reward processing, as

implied by pharmacological and DA depletion studies (May and Wightman 1989; Meredith, Ypma et al. 1995). Definitive evidence for this model is lacking, and it has been sustained largely for lack of a more elegant explanation. Even more complicated arrangements have also been proposed, including the possibility that the directly stimulated descending fibers course through the VTA and terminate on cholinergic neurons in the PPTg, which in turn synapse on DAergic neurons in the VTA, which in turn ascend to the accumbens (Yeomans, Mathur et al. 1993). Based on the repeated inability to definitively disrupt the rewarding effects of BSR by focal lesions of any particular brain structure or fiber pathway, others have argued that the substrate for BSR is in fact a diffuse "net-like" neural architecture (Simmons, Ackermann et al. 1998).

With this cloudy picture of the circuit architecture underlying BSR in mind, we decided to test the effects of focally blocking activity in the VTA on the network activation in response to BSR. If reward depends on the descending fibers to the VTA, which are subsequently broadcast rostrally, we would expect that blocking activity in VTA would interfere with normal reward signaling in rostral brain regions, such as the NAc. We implanted rats with both a stimulating electrode in the MFB, and with a cannula placed just dorsal to the VTA. After training these rats in the operant paradigm and obtaining psychometric curves, we imaged the whole-brain activation in response to BSR before and after pharmacological inactivation of the VTA. We infused a mixture of lidocaine (sodium channel blocker) and gadolinium into VTA. Gadolium is a non-toxic MRI contrast agent which allows us to visualize the spread of injection. We took images during an injection period that lasted for ten minutes prior to re-initiating the stimulation protocol, and display the injection spread overlaid on the structural image of a slice

through the VTA (Figure 17a). BOLD activity in the area of the injection spread, including the VTA and the SN, is completely abolished by the injection (Figure 17b).

When we compare the activity in the brain before and after the infusion of lidocaine, the most heavily silenced regions, other than VTA and SN, is the contralateral hemisphere of the brain (Figure 17c). Areas including the contralateral thalamus, caudate putamen, and sensory cortices are the most strongly affected. The only contralateral brain region showing an increase in activity during VTA silencing is the cingulate cortex. There is evidence that cells in SN and VTA have contralateral projections to the caudate putamen and thalamus (Douglas, Kellaway et al. 1987) and silencing these neurons may be partially responsible for the decrease in activity on the contralateral hemisphere. Another possible contributor to the dampening in activity in the opposite hemisphere is the presence of midbrain decussations near the site of inactivation. These axonal fibers might themselves be directly silenced by lidocaine as well.

On the other hand, a surprising effect resulting from VTA/SN inactivation is an increase in activity in some brain regions located in the ipsilateral hemisphere. Two notable areas that were previously found to track the behavioral reward magnitude response curve are also areas that show an increase in BOLD responses as a result of silencing VTA/SN. The strongest increases are in the amygdala, the shell of the nucleus accumbens, portions of the hippocampus and the piriform cortex. The strong overlap of these regions with the regions that were found to track reward magnitude (the NAc and amygdala) is intriguing. It suggests that the VTA/SN have a specific relationship with the distributed network that represents reward value. It does not appear that VTA itself

directly contains a representation of reward magnitude (see above). However, inactivating VTA disrupts the representation of reward magnitude in other brain regions. These results suggest that VTA plays a central role is coordinating reward magnitude representation in a suppressive modulatory manner.

If in fact VTA inactivation interferes with the representation or computation of reward magnitude in the brain, we should see alterations in the psychometric behavioral response curve when VTA is inactivated in the awake and behaving rat. In order to test the effects of silencing VTA/SN in the awake rat, we combined our already existing operant behavior paradigm with the ability to infuse a lidocaine/gadolinium mixture as used in the imaging sessions. We used a subset of three frequencies from the original set of ten frequencies used in prior experiments. The three frequencies were strategically chosen to capture the sigmoidal shape of the behavioral response curve measured previously and to reduce the duration of each behavioral session. After collecting response curves and observing that reward saturation occurred, lidocaine/gadolinium was infused into VTA ipsilateral to the stimulating electrode. Rats continued to nosepoke for BSR demonstrating that brain stimulation was still rewarding. As a result of silencing VTA/SN, the reward response curve no longer saturates (Figure 18). Instead, the relative number of nosepokes made at each frequency increases linearly with respect to frequency. In general, the percentage of choices made per frequency increases in comparison to the control behavioral data. By disrupting activity from VTA/SN, the ability to accurately attribute a reward value to a stimulus is corrupted. These data support the idea that the role of VTA is to modulate activity in the distributed network which represents reward magnitude value. Therefore, the

experience of reward *per se* is not critically dependent on VTA or SN afferents, but the mechanism for computing reward magnitudes is strongly affected.

FIGURES

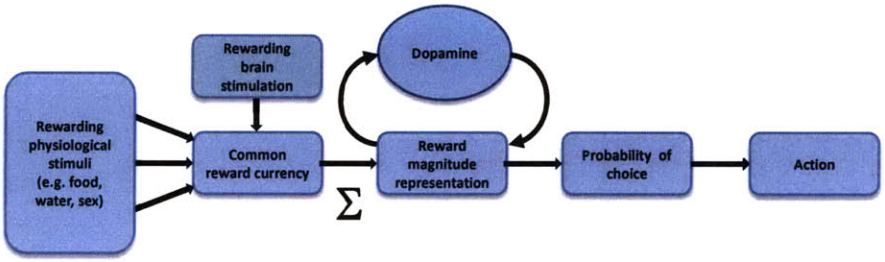

Figure 1. Schematic of decision-making process. Studies suggest that sensory and physiological input, as well as artificial rewarding electrical brain stimulation interact with similar neural circuitry. At the first stage, rewarding stimuli of different modalities are converted to a 'common reward currency', which serves as the primary input to following stages. Subsequently, the reward input is transformed into a higher-order representation of the value of different stimuli. A decision transformation (Herrnstein's matching law) maps this value representation onto the probability of available behavioral responses. At the final stage, this representation is reduced to a single behavioral choice. We propose that VTA, ventral tegmental area, the midbrain origin of the dopaminergic neurons, contributes a modulatory signal in the development of reward representation in this framework.

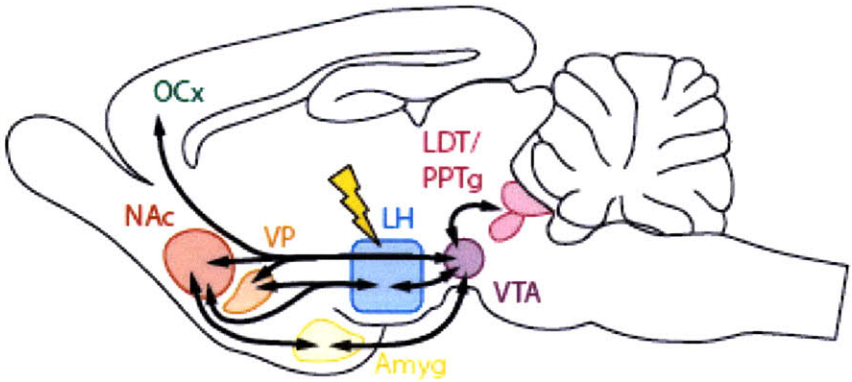

Figure 2. Brain circuits for reward. A schematic of ascending and descending connections of the dopamine mesolimbic pathway. VTA projections extended throughout the neural axis via the medial forebrain bundle. A majority of afferents to the nucleus accumbens (Nac) originate in VTA. Other areas in the basal forebrain and prefrontal cortices such as the ventral pallidum and orbitofrontal cortex also receive rich dopamine inputs. VTA also receives excitatory cholinergic inputs from areas in the brain stem (LDT/PPTg). Rewarding electrical pulses were delivered to lateral hypothalamus (LH in blue)

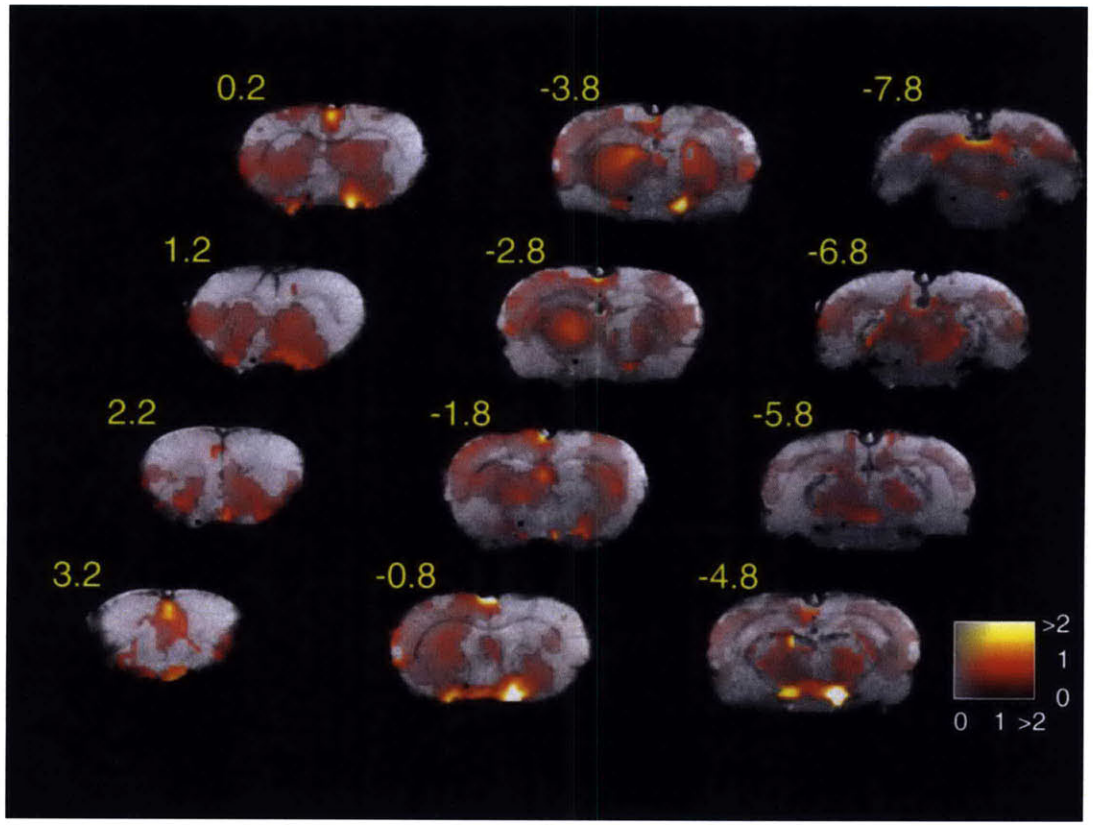

Figure 3. Rewarding stimulation-induced brain activity. Combined and co-registered data from ten animals. Rewarding electrical brain stimulation (BSR) delivered to the medial forebrain bundle at the level of LH induced BOLD responses in several brain areas ($p < 0.05$, Bonferroni corrected). Hotspots of activity are seen in regions ipsilateral to stimulation. Areas in the contralateral hemisphere were also significantly activated. Shown are twelve slices in the coronal plane at 1mm intervals from 3.2 to -7.8 relative to bregma (indicated above each slice). The background image is the anatomical T-2 weighted structural image. Overlaid is a map of the magnitude of response of significantly activated voxels. Transparency of each voxel is determined by the strength of activation, according to the colorbar.

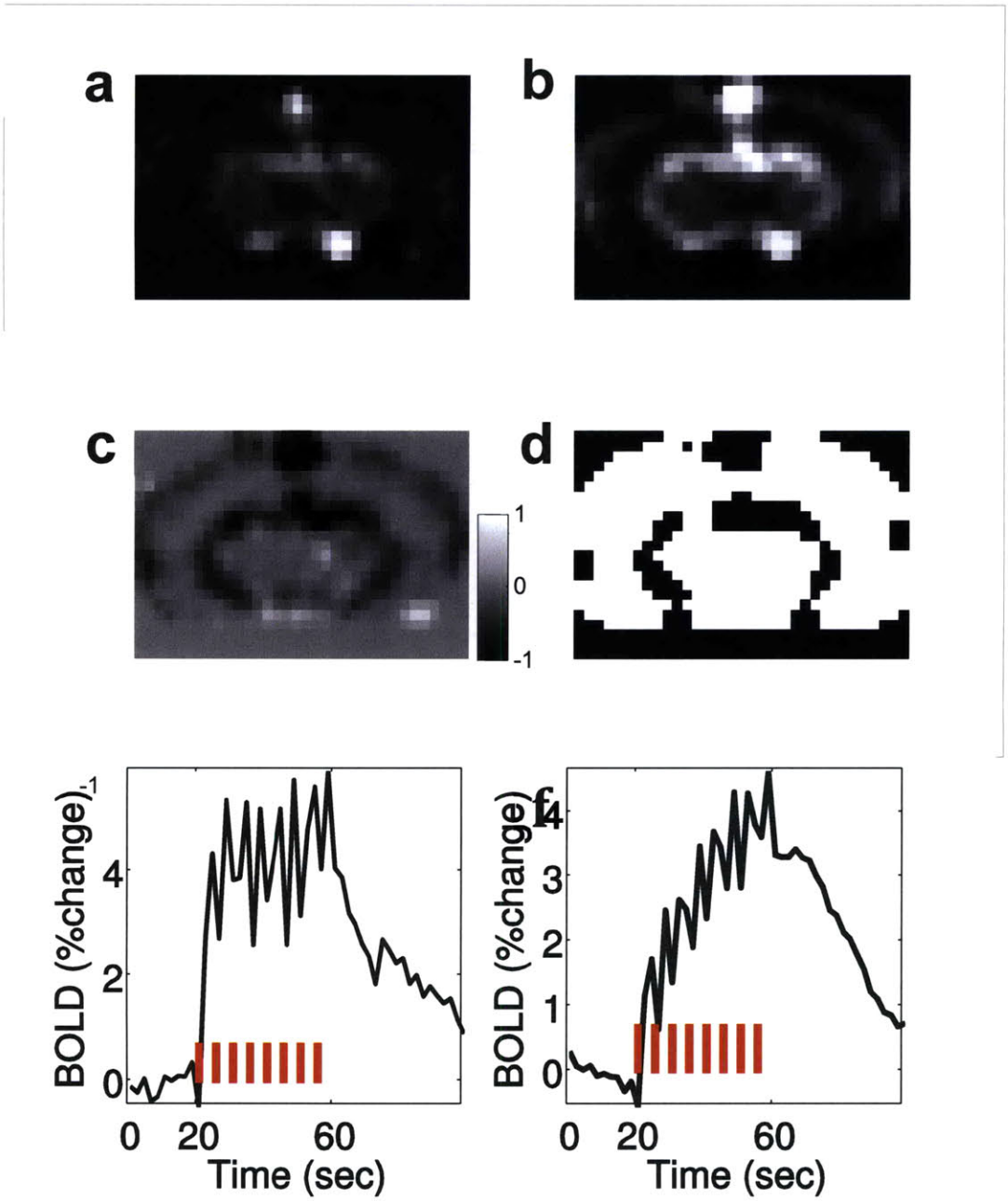

Figure 4. Removal of BOLD responses resulting from large draining vessels. a. Map of response magnitude from an example slice, calculated from the first two trains in the cycle. b. Maps of response magnitude, calculated from the last two trains in the cycle. c. Map of the difference between the activity elicited by the first two trains and the activity elicited by the last two trains. Note that areas with larger responses to the later trains appear darker. d. Mask of the voxels with substantially larger response to the late trains than to the early trains, indicative of contamination from large draining vessels. e. Time-course of response to one stimulus cycle , taken from the voxels determined to be highly contaminated by large draining vessel responses. Each stimulus cycle consisted of a sequence of eight stimulus trains (denoted by the vertical red hash marks), each lasting one second, with four seconds between. Note that the response increases incrementally with each train in the cycle). f. Time-course of the response in the pre-optic area (PO). Note that each train elicits a discernable increase in activity.

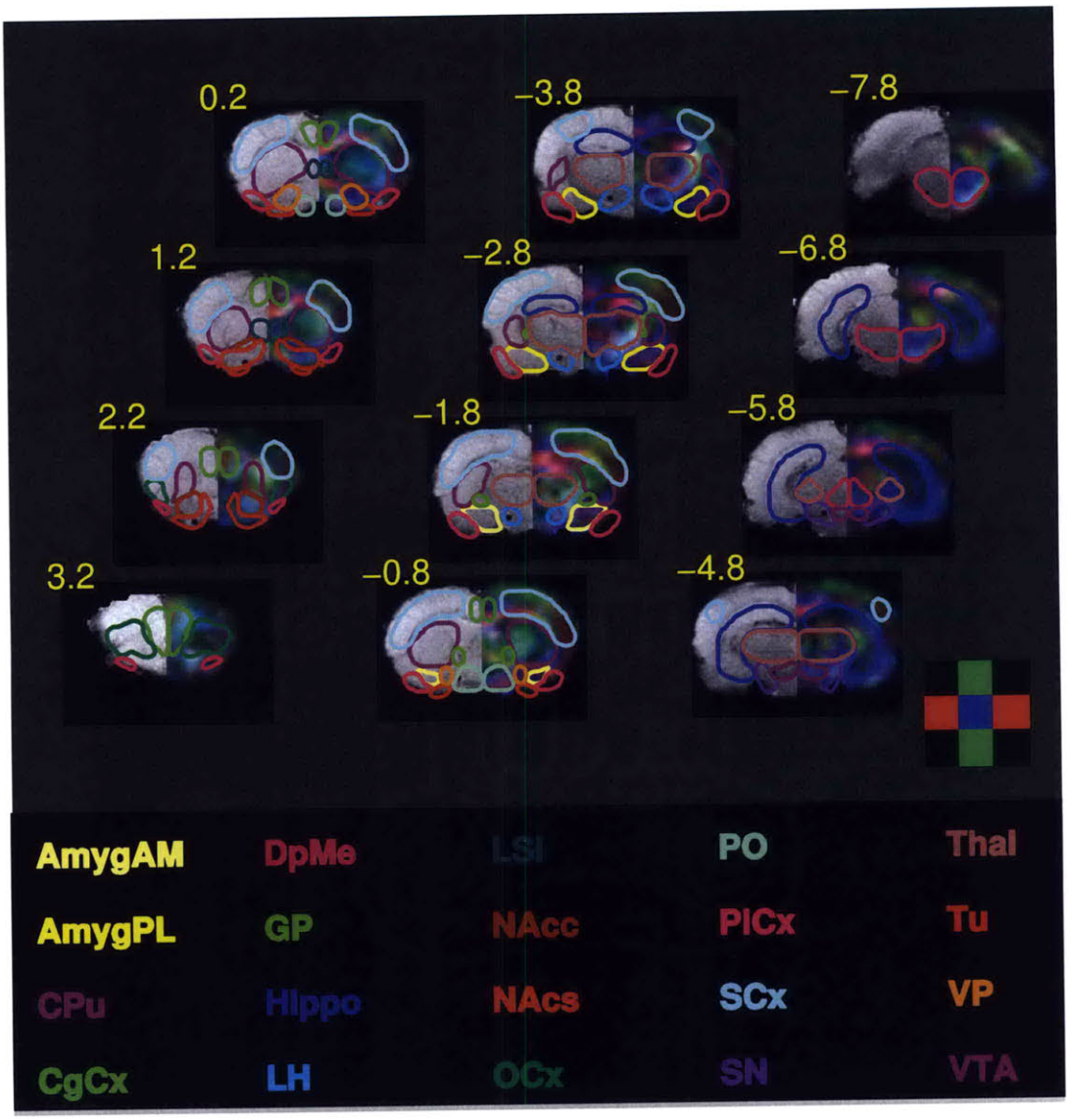

Figure 5. ROIs defined by DTI and anatomical scans. Regions of interests (ROIs) were defined with the aid of diffusion tensor imaging (DTI; right hemisphere), high resolution anatomical images (left hemisphere), and the Paxinos brain atlas. DTI maps enabled the visualization of axonal fiber tracts in the brain which provided valuable anatomical landmarks. Twelve coronal brain slices, arranged as in Fig 3. Red indicates orientation of fiber tracts left-to-right, green indicates up and down, and blue indicates in and out of the plane of the image. Color-coded ROIs are overlaid on the structural maps.

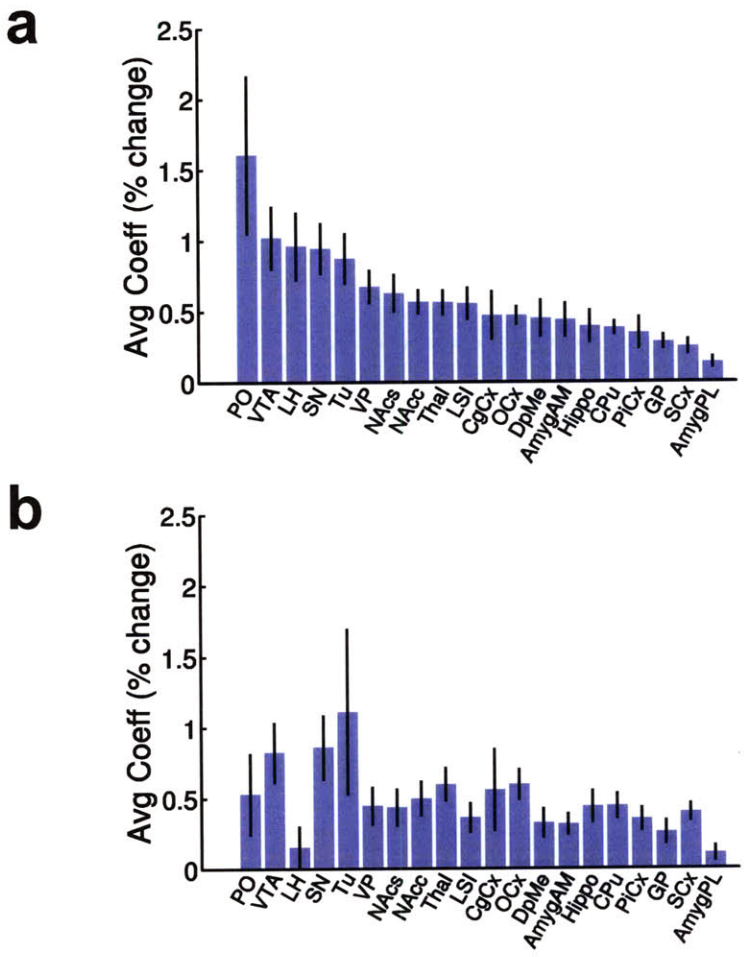

Figure 6. ROI analysis of response magnitude. a. Mean BOLD response within each ROI (all voxels) on the hemisphere ipsilateral to site of stimulation. The largest responses are found in the ventral areas of the brain, many of which are along the mesolimbic pathway. b. Mean normalized BOLD response in the hemisphere contralateral to site of stimulation. In general, the responses are smaller contralaterally. The largest differences are in ventral areas that receive direct projections from the MFB.

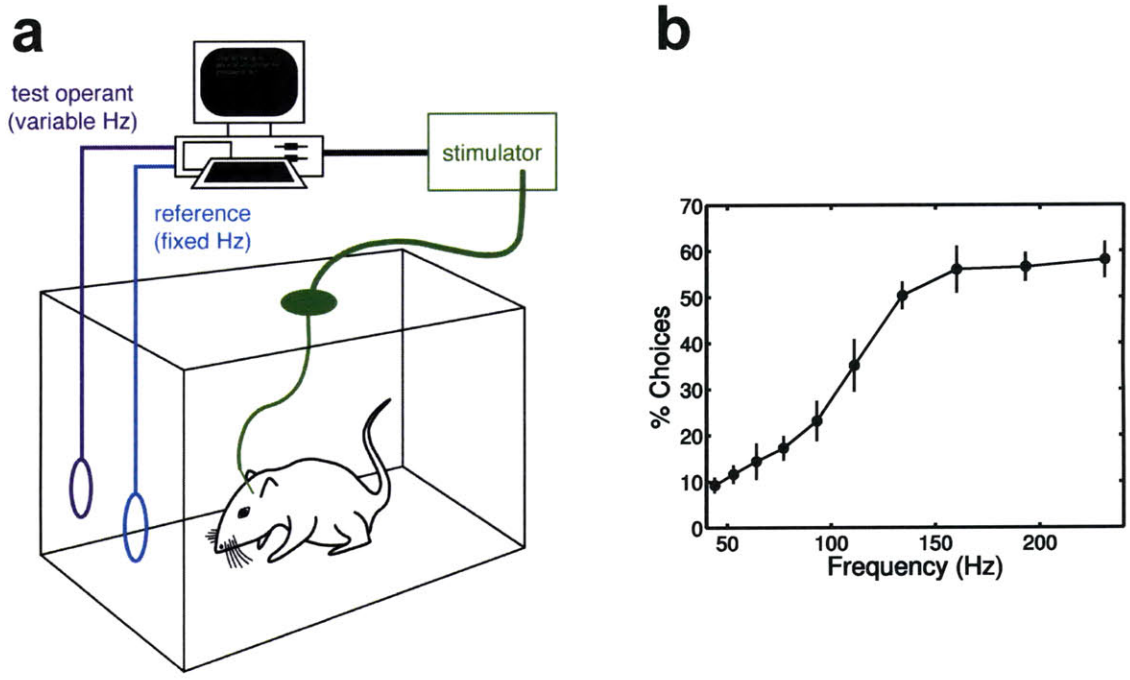

Figure 7. Behavioral assessment of reward magnitude. a. Schematic of rat training chamber. Rats are presented with a two-choice task (each option is represented by a circle). Nosepoking triggers the computer to send rewarding brain stimulation of a frequency depending on the option chosen. One nosepoke will always be a fixed frequency while the other changes from trial to trial. b. Titration curves measured from ten animals trained to receive brain stimulation rewards: Results from several sessions (described in the Methods) were averaged to obtain the mean percentage of choices made at each comparison frequency. This percentage reaches an asymptote of 50%, at comparison frequencies above 134Hz, indicating that higher stimulation frequencies are no longer preferred to the reference (150Hz). Error bars denote standard error of the mean.

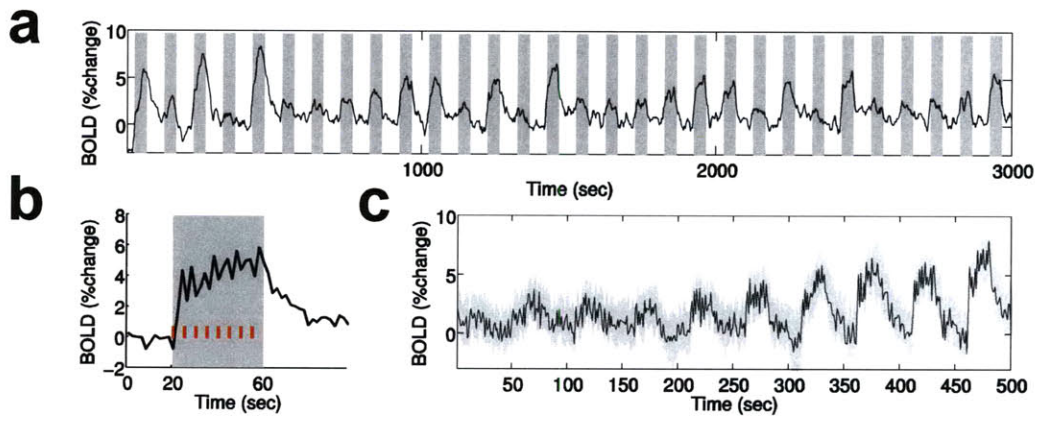

Figure 8. BOLD responses to the multiple frequency stimulus protocol
a. Time-course of BOLD activity changes in the lateral hypothalamus (LH) in response to the sequence of stimulus frequencies, presented in pseudo-random order. Each of ten frequencies was presented three times. Variable amplitudes of response are clearly visible. **b.** Averaged response to one cycle of the stimulus. **c.** Averaged responses to each stimulation frequency, rearranged in ascending order of frequency.

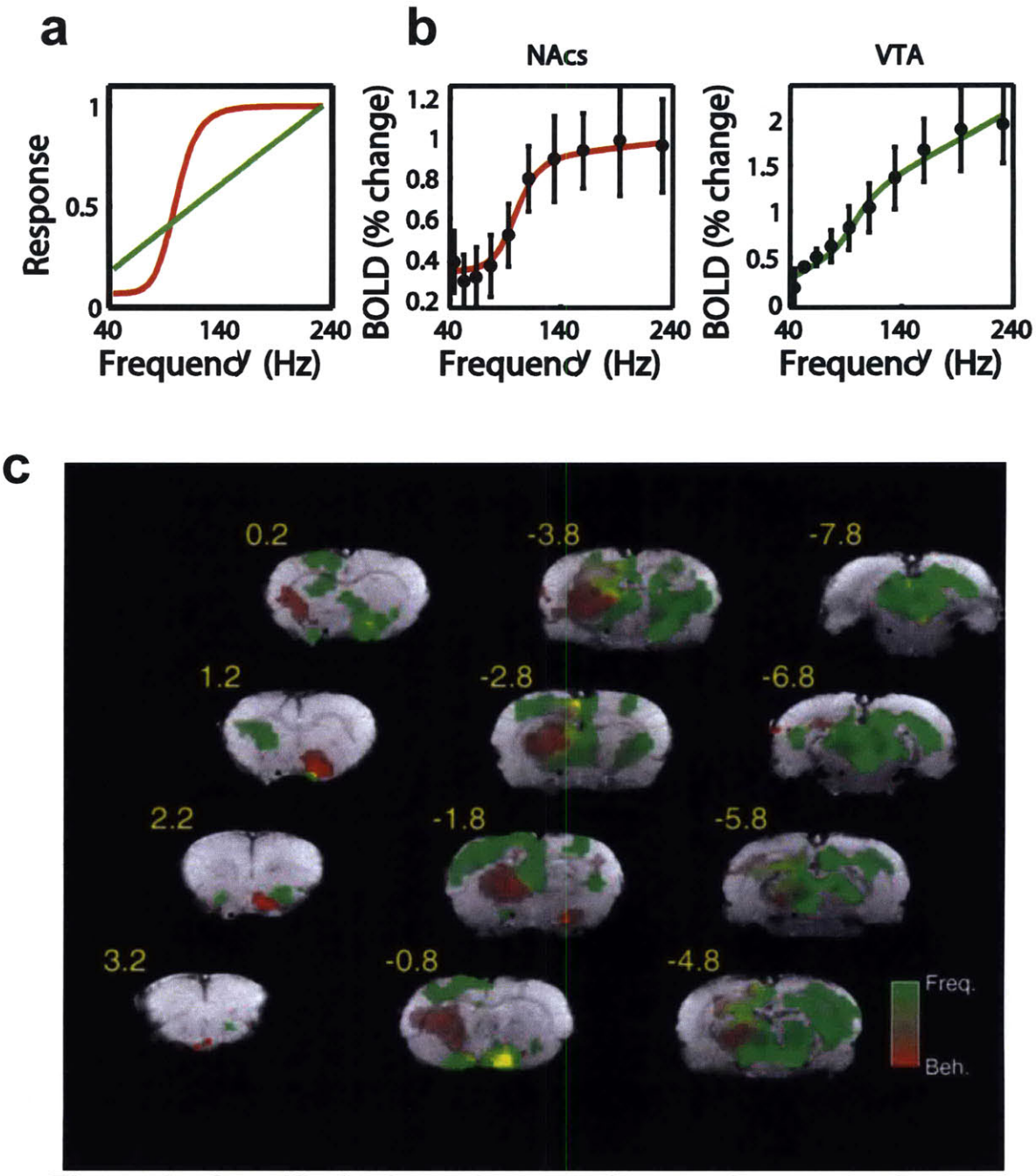

Figure 9. Specific brain regions track reward magnitude. a. Plot of the two factors used in the model of frequency-response curves. The red curve is the idealized behavioral reward curve. The green curve represents a linear response to stimulation frequency. These two regressors were used to distinguish reward-tracking voxels from linear voxels. b. Average frequency-response curves from two brain regions, the nucleus accumbens shell, and the ventral tegmental area (VTA) are shown by open circles. Error bars indicated uncertainty estimated from a Jack-Knife analysis. The lines represent the best fit of the model (linear combination of the two regressors in b). The color of the fitted curve denotes whether the behavioral regressor was significant (red) or the linear regressor was significant (green). c. Maps of the behavioral vs linear model comparison, as described in a-b. Voxels that were significant for the behavioral regressor are shown in red, significant for the linear regressor in green, and voxels with significant contributions from both are shown in yellow.

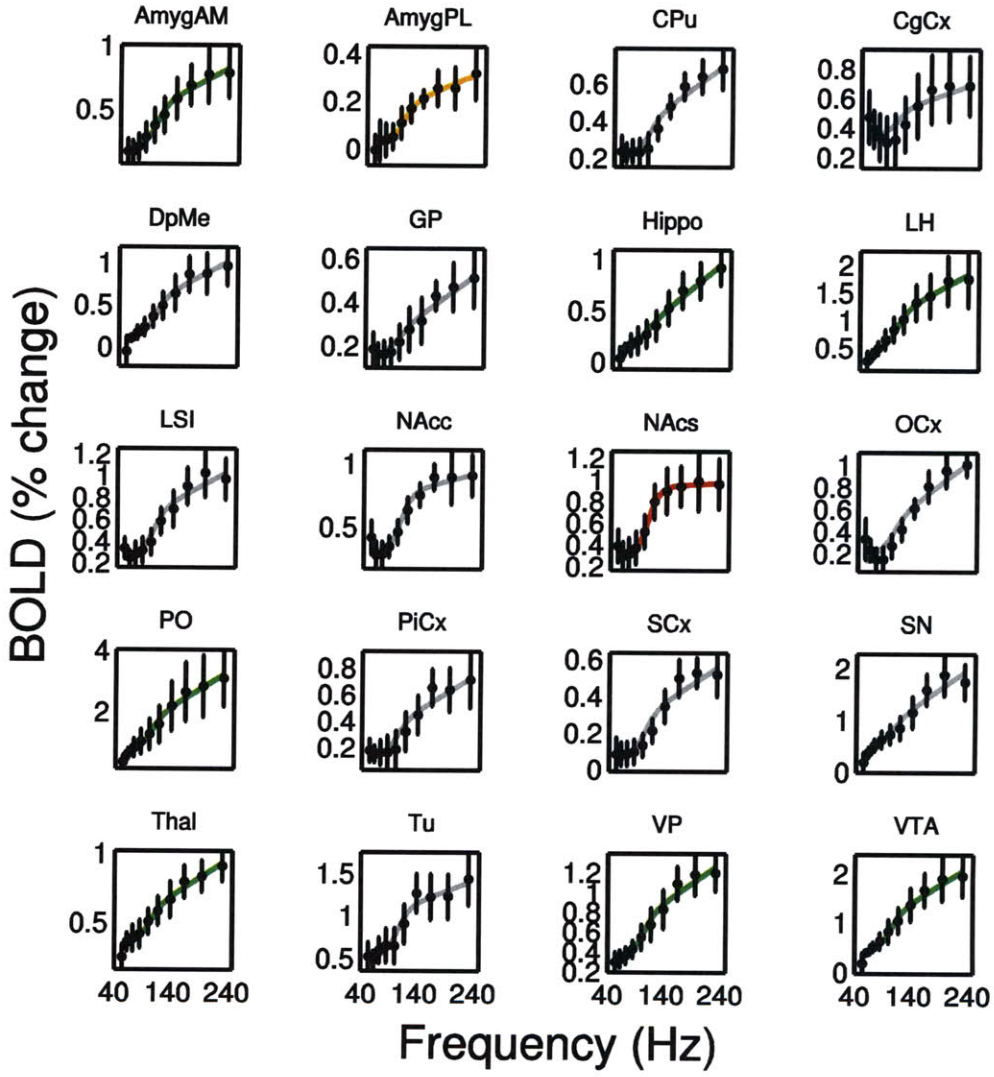

Figure 10. Specific brain regions track reward magnitude. Average frequency-response curves from each brain region are shown by open circles. Error bars indicated uncertainty estimated from a Jack-Knife analysis. The lines represent the best fit of the model (linear combination of the two regressors in Figure 12a. The color of the fitted curve denotes whether the behavioral regressor (red), the linear regressor (green), both (gold) or neither was significant.

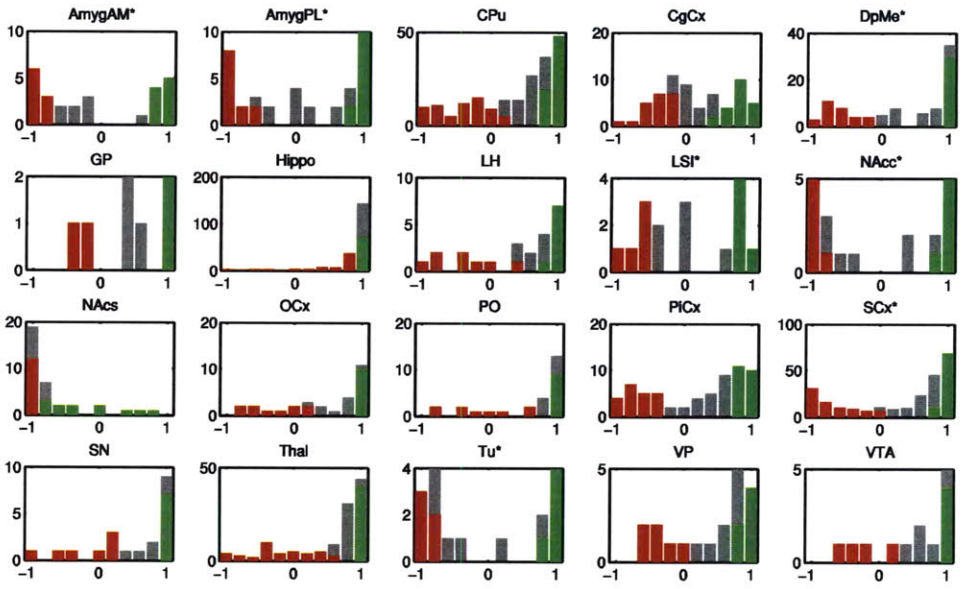

Figure 11. Some ROIs have bimodal distribution of linear and saturating voxels. Histograms of the distribution of the relative ratio of behavioral and linear T-statistics for all the voxels in each ROI. Values approaching 1 indicate that the voxel is highly significant for the linear regressor and poorly explained by the behavioral regressor. Values approaching -1 indicate that the voxel is highly significant for the behavioral regressor, and poorly explained by the linear regressor. The top 33% most linear voxels are shown in green, and the top 33% most behavioral voxels are shown in red. The p-values of the Hartigan Dip Test for bimodalty are shown above each plot. Some brain regions (e.g. the AmygAM) are bimodal, whereas others (e.g. the Nacs and the Hippo) are unimodal. A bimodal distribution within a brain region suggests that subregions may have functional differences in reward magnitude representation.

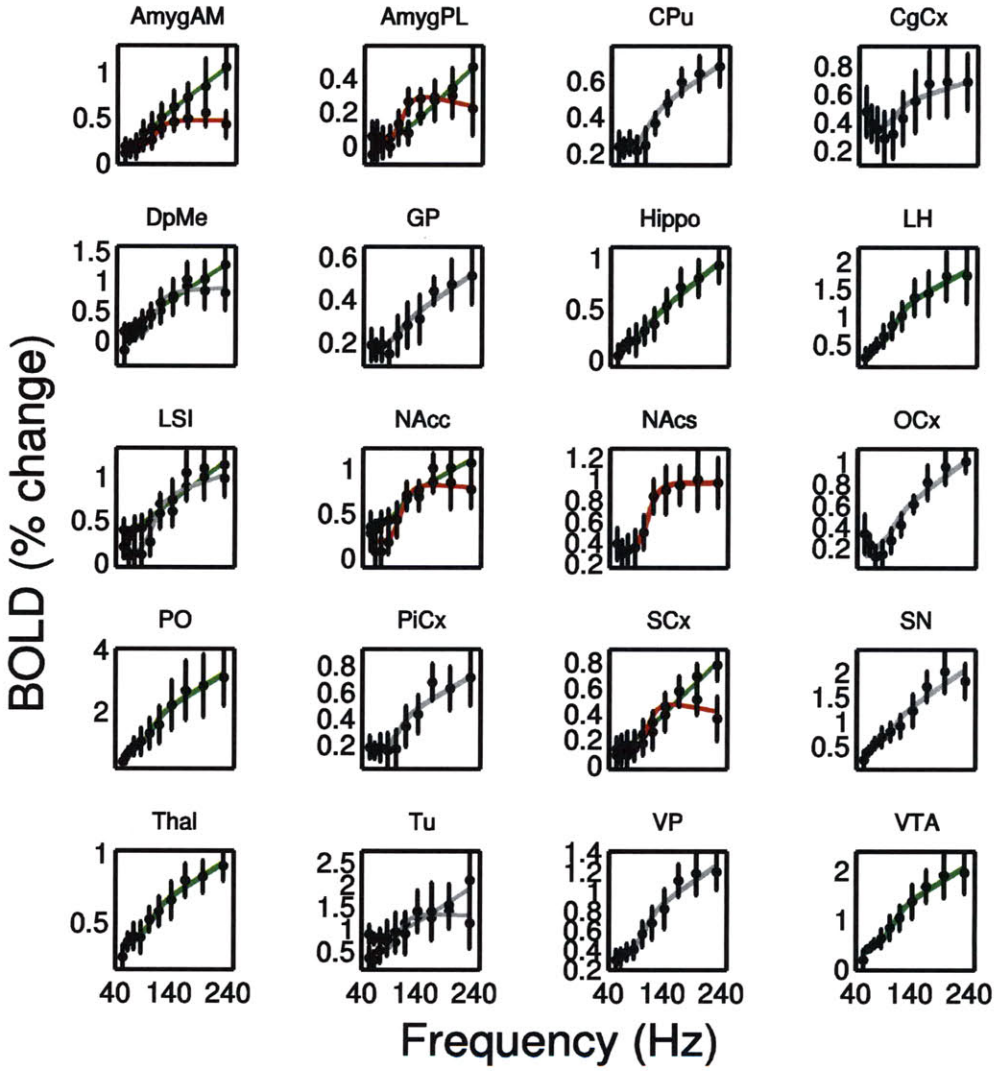

Figure 12. ROI curves of sub-regions of bimodal ROIs. Average frequency-response curves from sub-regions of each brain region are shown by open circles. Conventions are identical to Figure 13. Significantly bimodal ROIs were subdivided into the top 33% most linear and top 33% most behavior-tracking, and curves were computed from these two sub-populations independently. ROIs that were not significantly bimodal were not subdivided.

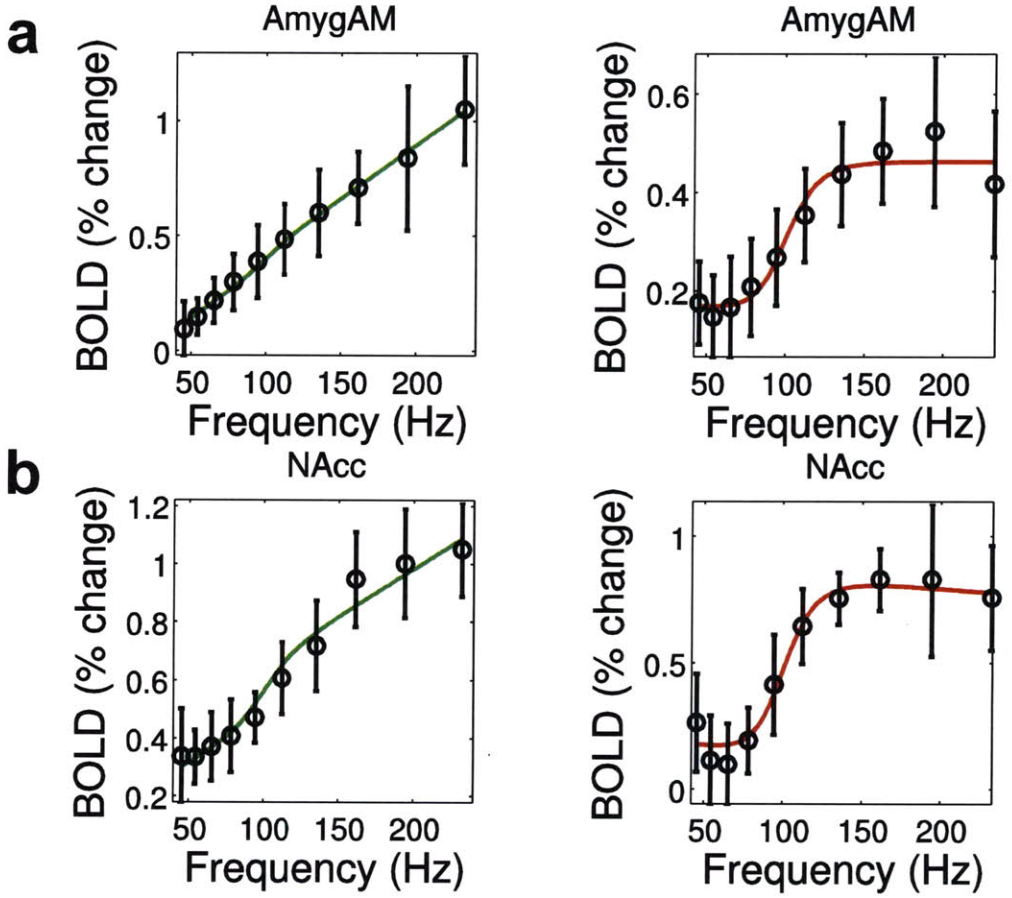

Figure 13. Behavior-tracking components of bimodal ROIs. a. Reward frequency curves for the two sub-populations of voxels in the AmygAM. Left panel shows the average curve from the top 33% of linear voxels within the ROI. Right panel shows the top 33% most saturating voxels. b. Similar curves to a. computed from the NAcc.

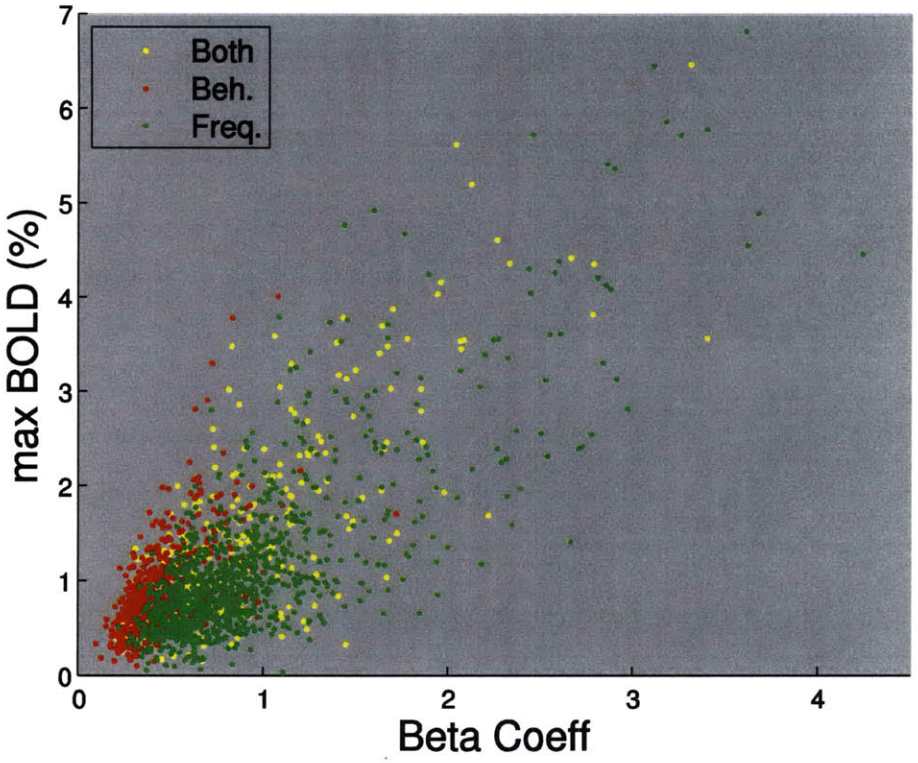

Figure 14. Response saturation of voxels does not result from saturation of neurovascular coupling. Scatterplot of the maximal BOLD response amplitude as a function of the weight of the Beta coefficient magnitude from the GLM fit.

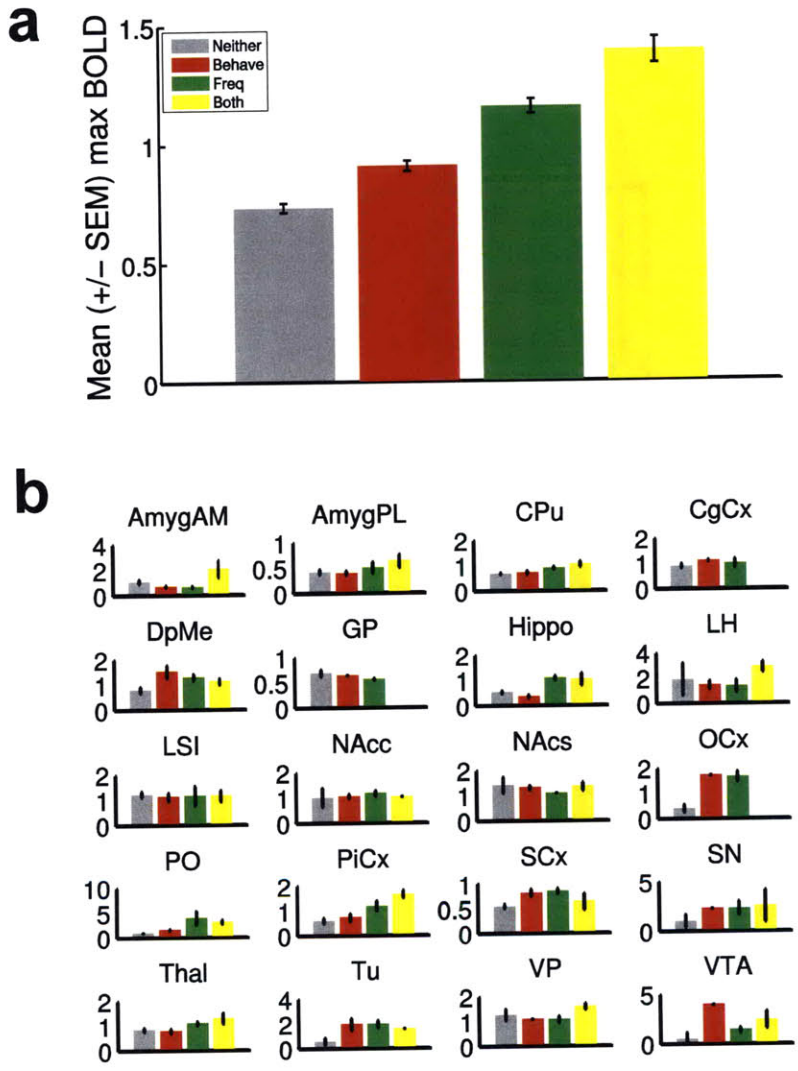

Figure 15. Response saturation of ROIs does not result from saturation of neurovascular coupling. Comparison of maximal BOLD response amplitude for ROIs that were significantly fit by behavioral or linear response curve regressors. a. Bar graph of the average (+/- SEM) maximal BOLD response for all voxels, categorized by the significant contribution of the two regressors according to the legend. b. Same analysis as in a, calculated individually for the voxels in each ROI.

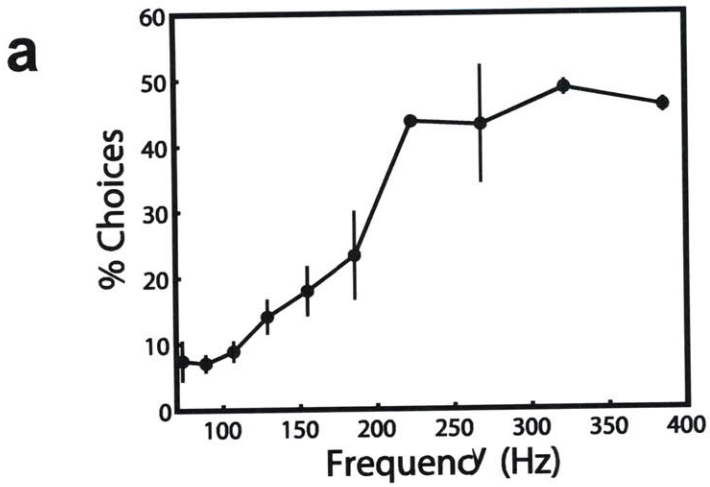

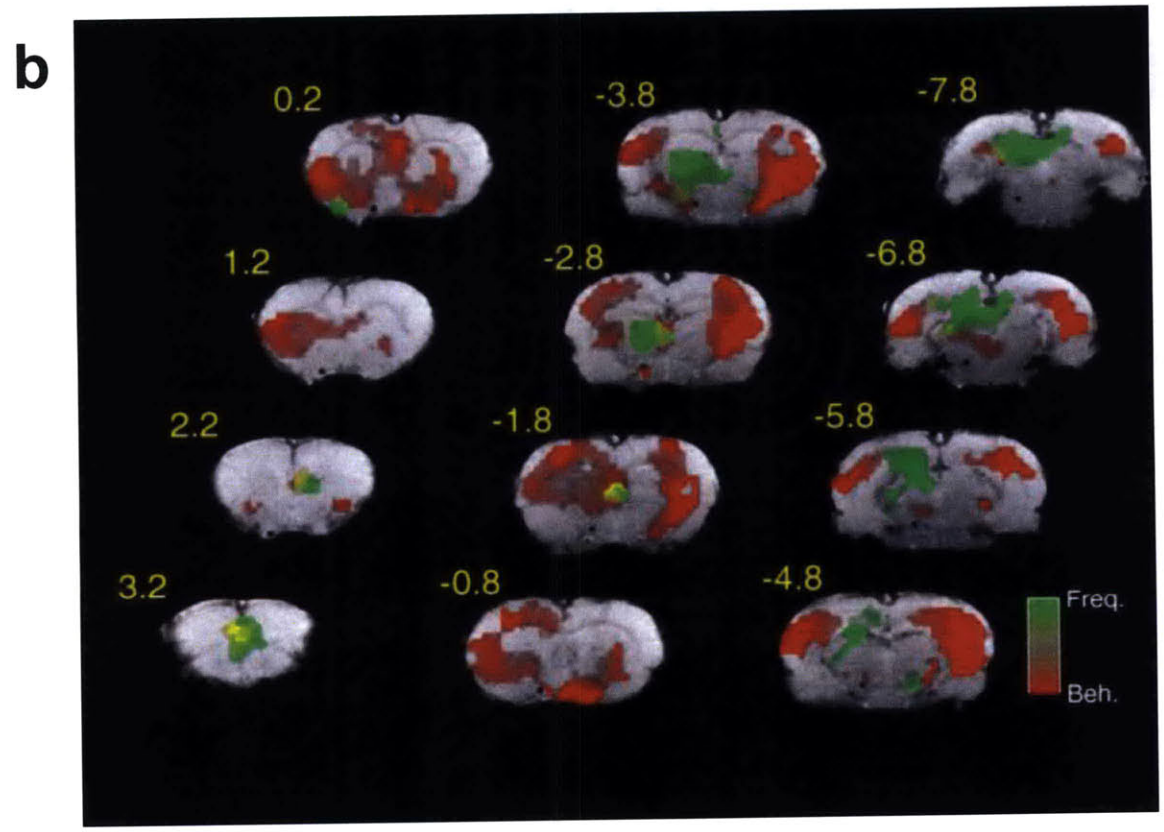

Figure 16 BOLD saturation with high frequency stimulation. a. Average (+/- SEM) behavioral response curve measured from two rats using a set of higher frequencies. The curve saturates above ~223Hz, likely due to faiure of axons to follow stimulation frequencies faithfully. b, Maps of the results of the regression analysis from this high frequency stimulation protocol. The curves from the majority of voxels were best modeled by the behavioral regressor, indicated in red.

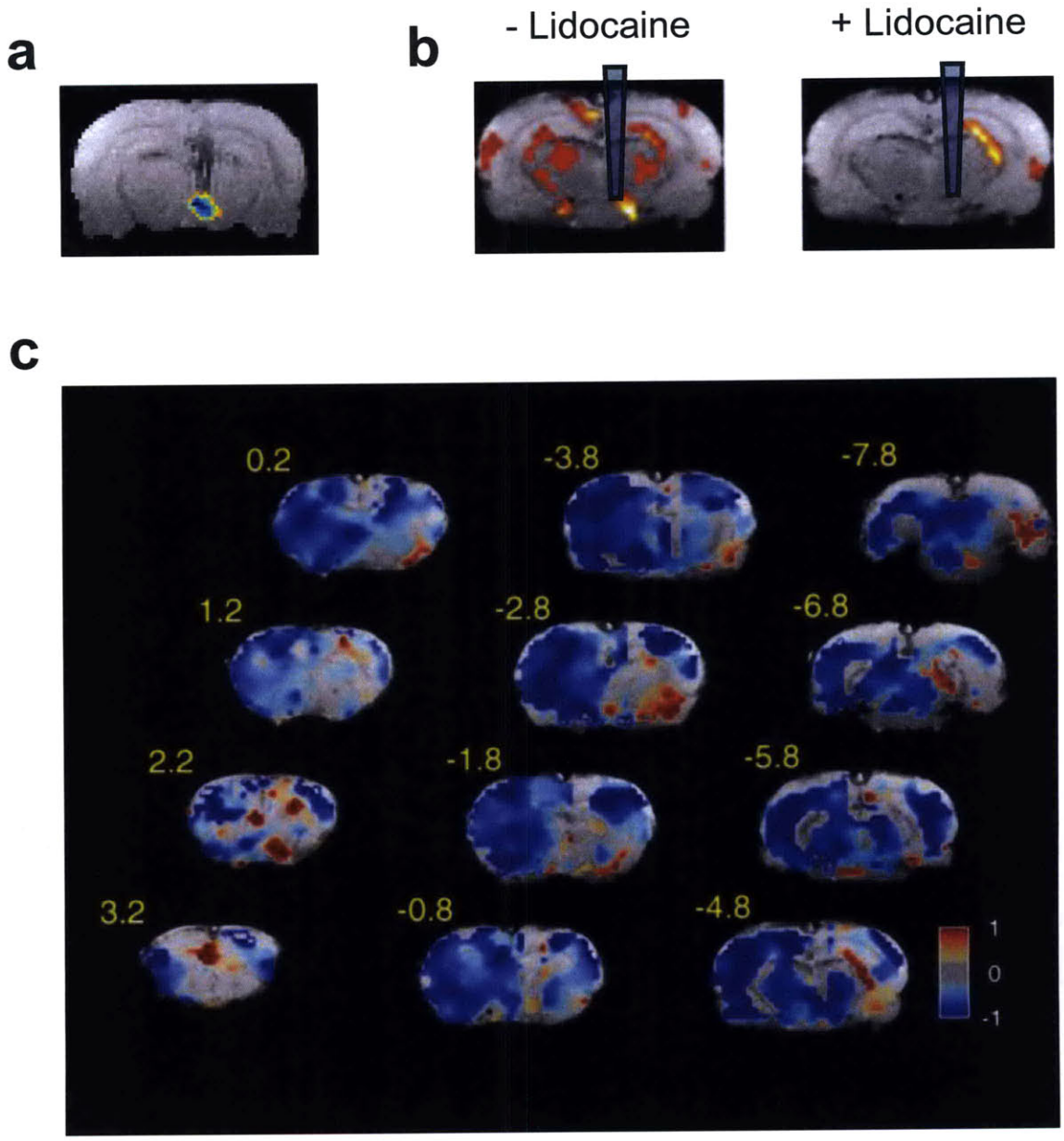

Figure 17. Inactivation of VTA disrupts neural reward value representation. a. Spread of the lidocaine injection, visualized by the spread of the co-injected gadolinium. Background image is the structural image obtained from the FSE scan. Note that the position of the injection cannula is visible. Overlaid is a pseudo-colored representation of the change in image brightness between post-injection and pre-injection. The apparent spread of the injection has a radius of ~1mm, and includes the large majority of the VTA. b. Stimulus-evoked amplitude maps from the pre- and post-lidocaine injection scans. The approximate location of the injection cannula is indicated. Note that the activity in the vicinity of VTA is completely abolished by the injection. c. Maps of the change in amplitude for the response to the highest frequency, following lidocaine inactivation of the VTA.

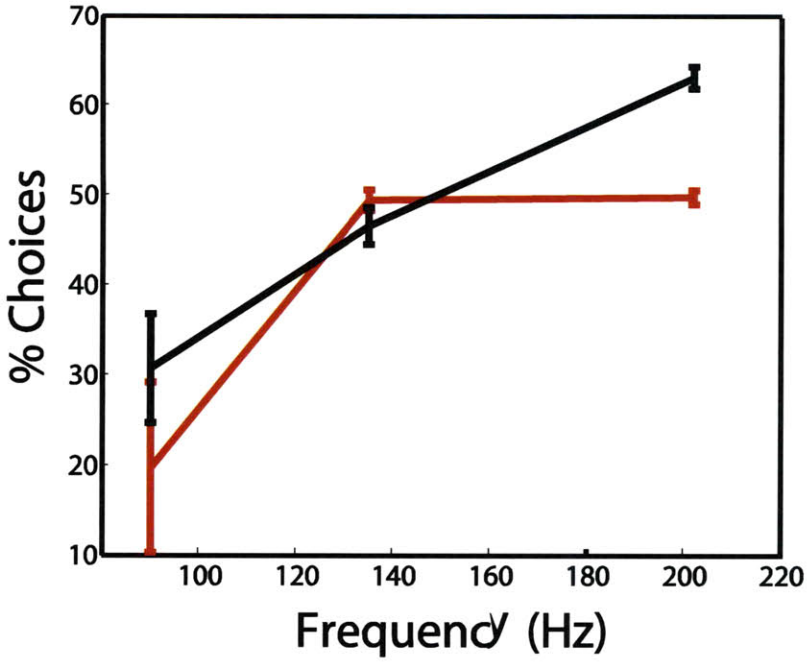

Figure 18. Inactivation of VTA disrupts normal behavioral reward matching. Behavioral frequency-response curves (n = 3) taken before (red) and after (black) lidocaine inactivation of the VTA.

DISCUSSION (CHAPTER 3)

Overall conclusions

The psychological concept of reward is fundamental to an animal's ability to make decisions, learn from their outcomes, and adaptively interact with the external world. Psychological studies have thoroughly described many aspects of behavior that are related to reward. However, the neural underpinnings of reward remain vaguely understood. Due to the fundamental necessity of the reward system, the brain circuits involved are built upon some of the evolutionarily oldest brain structures in the midbrain. In part, the difficulty in disentangling the complex anatomical wiring of the reward circuit derives from this fact. In part, the lack of understanding also arises from dearth of appropriate methodological approaches to understanding the system. In this thesis, we have addressed the representation of reward in the brain by combining the classic approach of rewarding electrical brain stimulation with modern circuit dissection tools, including high resolution measurements of BOLD activation, diffusion-tensor imaging and a local pharmacological silencing *in vivo*. Using these tools, we have addressed the following three specific aims.

Identifying neural elements activated by rewarding electrical brain stimulation of the medial forebrain bundle

Our first aim was to delineate the brain regions that are activated by rewarding electrical brain stimulation of the MFB. In other words, we wished to outline the neural circuit that could plausibly be involved in the direct representation of reward value. Not surprisingly, given the anatomical connectivity of the projections through the MFB, we

observed widespread activation along nearly the entire rostro-caudal axis of the brain. Though many structures had significant activity, the pattern of response magnitude was instructive. We found several distinct hot-spots of particularly large activity along the ventral-medial aspect of the ipsilateral hemisphere, including the pre-optic area, the substantia nigra, the VTA and the olfactory tubercle. However, there was significant activation in many additional brain structures. There was also a surprising level of activation in the contralateral hemisphere. The contralateral activity was generally diffuse and devoid of distinct hot-spots.

These results confirm several of the findings from previous experiments using other methods to identify brain regions activated by BSR, including c-fos labeling and 2-deoxyglucose labeling. Similarly to experiments using c-fos and 2DG labeling, our data show bilateral activation in several areas including the thalamus, nucleus accumbens, lateral septum, and in sensory and motor cortices (Porrino, Esposito et al. 1984; Arvanitogiannis, Flores et al. 1996). These studies report that some of the largest differences in activity between areas ipsilateral to stimulation versus contralateral are rostral-caudal targets of the MFB, for example the preoptic area as well as the substiantia nigra and VTA. As is visible in Figure 3, a majority of activation hotspots are ispilateral to stimulation and are localized in the preoptic area, lateral hypothalamus, and the VTA/SN. Our mapping of the activity induced by rewarding stimulation is in strong agreement with the existing literature. Yet, many of the papers aiming to elucidate the neural substrates of rewarding brain stimulation provided inconclusive results, mainly due to the limitations of their techniques. They rely on metabolic

markers that could only give them a measure of regions that were active during stimulation whether or not those regions played a significant role in reward.

Identifying structures that represent reward magnitude

The reward system must have the ability to finely discriminate different magnitudes of reward. Reward valuation has been well documented behaviorally, in the context of a number of rewarding stimuli, including sucrose, addictive drugs, and rewarding brain stimulation (Gallistel and Leon 1991; Di Chiara, Bassareo et al. 2004; Roitman, Stuber et al. 2004). These studies have demonstrated that animals will faithfully make choices based on the perceived reward value of the available options. The relationship between the relative allocation of choices and the reward value of the options has been formalized by Herrnstein, and found to apply universally across environment, task and species (Herrnstein 1974). An important aspect of this behavior is that animals do not maximize reward by always choosing the most rewarding option. Instead, they allocate time and action proportionally, according to reward value. The decision-making machinery responsible for this behavior must therefore have access to a quantitative representation of the reward magnitude of each option.

Our second aim was therefore to identify brain structures with activity levels that track the reward magnitude of varying frequencies of electrical brain stimulation, and thus identify the neural representation of reward magnitude, or value. We first confirmed previous results demonstrating that in a two-choice operant task rats will allocate choices in a graded fashion relative to the frequency of electrical brain stimulation (Waraczynski, Stellar et al. 1987; Simmons and Gallistel 1994). Based on this behavioral measure, we can assign a reward value to each frequency by calculating

the proportion of choices for each frequency, and generate a curve of subjective reward magnitude. An important aspect of the observed reward magnitude curves is that they do not linearly follow stimulation frequency. Rather, reward has a saturating relationship to stimulation frequency, with acceleration over low frequencies, and plateaus at high frequencies. Based on models of reward integration, it has been proposed that the saturation of the reward curve represents a practical limit to the possible perceived reward magnitude, not a biophysical saturation of the neural machinery (Shizgal 1997). Regardless of the mechanism, the reproducible reward curve profile provided us with a unique signature of reward magnitude which we used to distinguish brain activity related to the computation or representation of reward magnitude from other activity related linearly to the stimulation frequency.

We found that the majority of the stimulation-evoked brain activity linearly tracked the stimulation frequency. This is perhaps not surprising, given that neural activity can track the stimulation frequencies used, and previous studies have found that BOLD activation in the hippocampus linearly correlates with neural activity at least up to 50Hz (Canals, Beyerlein et al. 2008). There are two principal interpretations for why a voxel would have a linear response profile. One is that the voxel processing reward-related activation of the BSR, but that it is not directly involved in the reward magnitude representation. In the context of the reward integrator model of BSR (Shizgal 1997), it is conceivable that the integrator is several synapses removed from the directly stimulated fibers, and thus the BSR-evoked activity could propagate linearly through several synapses before reaching the reward integrator, which would count the number of spikes, and generate a sigmoidal reward curve. A second interpretation of linear

activity profiles is that some brain regions may be incidentally stimulated which are completely unrelated to the reward system. The MFB is an exceedingly complex fiber bundle, which contains many fibers with no role in reward. It is most likely that at least some non-reward fibers are stimulated, and lead to activation of voxels in brain regions with no role in reward. Unfortunately, we are not currently able to distinguish between these possibilities with the present experiments. A clear dissociation of non-reward-related activation will likely have to wait for more genetically and anatomically specific means of stimulation, such as genetically targeted expression of optogenetic probes.

We did identify two brain structures with activity profiles that clearly tracked the reward curve: the NAc and subregions of the amygdala. The extremely close relationship between the activation curves in these areas and the psychometrically derived reward curve make it extremely unlikely that the activity in these regions is anything other than reward magnitude tracking. Thus, our main conclusion for this aim is that the nucleus accumbens and the subregions of amygdala are the two major components of a distributed representation of subjective reward magnitude.

Several additional brain regions contained activity that is suggestive of a role in reward magnitude processing or representation. While large portions of the NAc and sub-populations in the amygdala were reward tracking, and met all of our criteria for significant tracking of the behavioral reward curve, several other brain regions (LSI, DpMe, Tu, SCx) showed a lesser degree of reward-tracking behavior. Each of these regions was found to have a bimodal distribution of linear vs. saturating voxels in the model fits. However, they neither had obvious spatial clustering of the saturating voxels, nor passed the stringent, Bonferroni-corrected test for a significant fit by the

saturating regressor within the sub-population that we extracted. While our criteria for this determination (including the extraction of 1/3 voxels) seem reasonable, they are somewhat arbitrary in functional terms. If a subregion smaller than one third of the volume of the brain structure had a specific functional role, it might have been washed out by our analysis. Similarly, if a fraction of neurons with a specific functional role were distributed throughout the structure, our analysis would likely have missed them, due to the limited spatial resolution of our method. Thus, we can tentatively say that these brain regions may be involved in the reward magnitude representation, but their role is not as central as those of the NAc and the amygdala.

Determining the role of the VTA in reward magnitude representation

Since early in the studies of the neural mechanisms of reward, there has been special attention paid to the role of the neurotransmitter dopamine in reward. Several pieces of circumstantial evidence have been accumulated to point to the role of dopamine in reward, and it has even been suggested that dopamine release in the NAc represent the reward signal itself (Yokel and Wise 1975; Wise 1982). The primary source of dopaminergic projections to the structures that we have identified as reward-tracking is the VTA. In fact, the VTA has widespread projections, and as such is well suited to coordinate the distributed reward value representation that we have observed. Our aim was to investigate the role of the VTA in the reward magnitude representation by selectively inactivating it during the presentation of BSR.

In order to address this issue, we developed a novel means of visualized focal inactivation. By mixing the MR contrast agent gadolimium (Gd-DTPA) with the nerve blocker lidocaine, we were able to directly visualize the spread of drug in the brain in

real time. This enabled us to carefully titrate the infusion parameters to generate a radius of inactivation that ensured complete inactivation of the VTA with only minimal unnecessary effects on nearby structures. We found this to be an indispensable tool, as we noticed unwanted spread (especially into the ventricles) in some pilot experiments. We were also able to readily identify failures of injection, which occasionally occurred due to minute leaks, or other technical failures. Presumably, other similar experiments performed without the visualization would have missed these issues, and have weakened, or non-specific effects.

We found that the inactivation of the VTA had widespread and varied effects on the brain-wide response to BSR. Not surprisingly, there was widespread reduction of BSR-induced activity, which was most prominent on the contralateral hemisphere. There are two principal interpretations of this finding. The first is that the neurons in the VTA send projections bilaterally. This would easily explain reduction in activity in the contralateral hemisphere, however quantitatively, it fails to explain why the reduction in the contralateral hemisphere was larger than in the ipsilateral hemisphere, given that only 20 percent of VTA projections are contralateral (Swanson 1982). The explanation that we favor is that two prominent decussations in the midbrain (the ventral tegmental decussation and the supramammilary decussation) are found at the level of the VTA (Douglas, Kellaway et al. 1987). Therefore, it is likely that the main gateways of descending activity elicited by BSR to the contralateral hemisphere were blocked by the inactivation of the VTA.

In the ipsilateral hemisphere, there was also a reduction in several brain areas, including sensory cortices and the caudate- putamen. Surprisingly, there were also

increases in activity along the ventral half of the brain. The largest increases were found in the amygdala, the NAc, the cingulate cortex and subregions of the lateral entorhinal cortex. Some of these areas are most strongly involved in the reward magnitude representation. This scenario suggests a striking conclusion: the brain regions which are the core of the representation of reward magnitude are suppressed by the VTA. Furthermore, it suggests that the VTA, while not directly involved in the representation of reward magnitude, has the ability to modulate, or shape, the reward value representation.

This conclusion led us to investigate the effects of inactivating the VTA on the behavioral read-out of reward magnitude. We found that inactivating the VTA disrupted the typical saturating reward profile, providing psychophysical confirmation that VTA plays a role in coordinating, or regulating the reward value representation.

There is abundant evidence for a modulatory role for DA from the VTA on glutamatergic and GABAergic inputs to the NAc (Nicola, Surmeier et al. 2000). It is currently believed that the dopaminergic inputs from the VTA are not drivers of NAc activity, but act strictly as modulators. The main excitatory drive to the NAc is thought to be glutamatergic inputs from frontal cortices, the amygdala and the hippocampus (Yim and Mogenson 1982; Yang and Mogenson 1984; Brady and O'Donnell 2004). In fact, the modulatory role of DA in the NAc is quite complex. There have been demonstrations that DAergic input can enhance or suppress NAc activity (Nicola and Malenka 1997), dependent on the membrane potential state of the NAc neurons.

Caveats

The basis of most fMRI experiments is the blood oxygenation level dependent (BOLD) effect. BOLD signals offer a useful but indirect readout of underlying neural activity. Therefore understanding the relationship between the hemodynamic response and the neural activity causing it is critical in order to interpret results accurately. Many experimenters have characterized the relationship between BOLD and direct measurements of neuronal activity such as local field potentials and multi-unit spiking activity. They demonstrate that there is a linear relationship between both measures given that the stimulus presented lasts for a short duration (Logothetis, Pauls et al. 2001; Hyder, Rothman et al. 2002). In addition, evidence shows that BOLD responses are better correlated with local field potentials suggesting that activation in an area likely reflects incoming input and local processing (Logothetis 2003). Therefore, based on the current understanding in the field, the results described in this thesis, which are based on changes in BOLD signals, are highly likely to reflect similar activation patterns due to underlying neural activity.

Furthermore, there is evidence that specifically demonstrates that there is a linear relationship between neural activity and BOLD activity during electrical brain stimulation. Canals et al., demonstrated that BOLD activation linearly follows neural activity during electrical brain stimulation of the hippocampus, over the range of frequencies tested (4 - 50Hz) (Canals, Beyerlein et al. 2008). Beyond that, our own data provide strong evidence in support of this conclusion. The simple fact that the majority of voxels have a nearly linear relationship to stimulation frequency over the entire range of stimulus frequencies used (up to 231Hz) strongly implies that the BOLD

activation is linearly related to neural activity. The stimulated axons in the MFB can readily follow frequencies up to ~250Hz (Forgie and Shizgal 1993). When we used the high-frequency regime, above the following-frequency of most MFB axons, we observed saturation of the BOLD throughout most of the brain, which presumably reflects a ceiling of the underlying neural activity. Taken together, we feel confident that the BOLD activity we observe is a reasonable surrogate for neural activity in our paradigm. Undoubtedly, subtle differences exist, but they are unlikely to influence the conclusions that we have drawn from the BOLD measurements.

Working Model

Integrating these results with what we know from the literature, we can begin to construct a hypothesis for the functional roles of different elements in the neural circuitry involved in representing reward value in the brain. The core representation of reward value is located in the ipsilateral NAc, and parts of the amygdala. This representation is enabled by modulatory inputs from the VTA/SN, which shape the reward-magnitude curve. The modulatory shaping is primarily due to suppression of responses to large reward magnitudes. Thus, ascending midbrain modulatory afferents have a role not only in learning reward associations, but also in modulating the reward value representation. This circuit arrangement provides a means by which the representation can be modified by other contextual factors that converge to influence the output of the VTA/SN.

References

Arvanitogiannis, A., C. Flores, et al. (1996). "Increased ipsilateral expression of Fos following lateral hypothalamic self-stimulation." Brain Res **720**(1-2): 148-54.

Bayer, H. M. and P. W. Glimcher (2005). "Midbrain dopamine neurons encode a quantitative reward prediction error signal." Neuron **47**(1): 129-41.

Berns, G. S., J. D. Cohen, et al. (1997). "Brain regions responsive to novelty in the absence of awareness." Science **276**(5316): 1272-5.

Berridge, K. C. and T. E. Robinson (1998). "What is the role of dopamine in reward: hedonic impact, reward learning, or incentive salience?" Brain Res Brain Res Rev **28**(3): 309-69.

Bielajew, C. and P. Shizgal (1986). "Evidence implicating descending fibers in self-stimulation of the medial forebrain bundle." J Neurosci **6**(4): 919-29.

Bishop, M. P., S. T. Elder, et al. (1963). "Intracranial self-stimulation in man." Science **140**: 394-6.

Boyd, E. S. and M. B. Celso (1970). "Effect of some brain lesions on septal intracranial self-stimulation in the rat." Am J Physiol **219**(3): 734-41.

Boyd, E. S. and L. C. Gardner (1962). "Positive and negative reinforcement from intracranial stimulation of a teleost." Science **136**: 648-9.

Brady, A. M. and P. O'Donnell (2004). "Dopaminergic modulation of prefrontal cortical input to nucleus accumbens neurons in vivo." J Neurosci **24**(5): 1040-9.

Canals, S., M. Beyerlein, et al. (2008). "Electric stimulation fMRI of the perforant pathway to the rat hippocampus." Magn Reson Imaging **26**(7): 978-86.

Chang, H. T., C. J. Wilson, et al. (1982). "A Golgi study of rat neostriatal neurons: light microscopic analysis." J Comp Neurol **208**(2): 107-26.

Cheer, J. F., B. J. Aragona, et al. (2007). "Coordinated accumbal dopamine release and neural activity drive goal-directed behavior." Neuron **54**(2): 237-44.

Conover, K. L. and P. Shizgal (1994). "Competition and summation between rewarding effects of sucrose and lateral hypothalamic stimulation in the rat." Behav Neurosci **108**(3): 537-48.

Cousins, M. S., J. D. Sokolowski, et al. (1993). "Different effects of nucleus accumbens and ventrolateral striatal dopamine depletions on instrumental response selection in the rat." Pharmacol Biochem Behav **46**(4): 943-51.

Day, J. J., M. F. Roitman, et al. (2007). "Associative learning mediates dynamic shifts in dopamine signaling in the nucleus accumbens." Nat Neurosci **10**(8): 1020-8.

Delfs, J. M., L. Schreiber, et al. (1990). "Microinjection of cocaine into the nucleus accumbens elicits locomotor activation in the rat." J Neurosci **10**(1): 303-10.

Di Chiara, G., V. Bassareo, et al. (2004). "Dopamine and drug addiction: the nucleus accumbens shell connection." Neuropharmacology **47 Suppl 1**: 227-41.

Douglas, R., L. Kellaway, et al. (1987). "The crossed nigrostriatal projection decussates in the ventral tegmental decussation." Brain Res **418**(1): 111-21.

Edmonds, D. E., J. R. Stellar, et al. (1974). "Parametric analysis of brain stimulation reward in the rat: II. Temporal summation in the reward system." J Comp Physiol Psychol **87**(5): 860-9.

Esposito, R. U., L. J. Porrino, et al. (1984). "Changes in local cerebral glucose utilization during rewarding brain stimulation." Proc Natl Acad Sci U S A **81**(2): 635-9.

Fields, H. L., G. O. Hjelmstad, et al. (2007). "Ventral tegmental area neurons in learned appetitive behavior and positive reinforcement." Annu Rev Neurosci **30**: 289-316.

Floresco, S. B., C. D. Blaha, et al. (2001). "Modulation of hippocampal and amygdalar-evoked activity of nucleus accumbens neurons by dopamine: cellular mechanisms of input selection." J Neurosci **21**(8): 2851-60.

Forgie, M. L. and P. Shizgal (1993). "Mapping the substrate for brain stimulation reward by means of current-number trade-off functions." Behav Neurosci **107**(3): 506-24.

Franklin, K. B. (1978). "Catecholamines and self-stimulation: reward and performances effects dissociated." Pharmacol Biochem Behav **9**(6): 813-20.

Gallistel, C. R. (1978). "Self-stimulation in the rat: quantitative characteristics of the reward pathway." J Comp Physiol Psychol **92**(6): 977-98.

Gallistel, C. R., G. A. Karreman, et al. (1977). "[14 C]2-Deoxyglucose uptake marks systems activated by rewarding brain stimulation." Brain Res Bull **2**(2): 149-52.

Gallistel, C. R., A. P. King, et al. (2007). "Is matching innate?" J Exp Anal Behav **87**(2): 161-99.

Gallistel, C. R. and M. Leon (1991). "Measuring the subjective magnitude of brain stimulation reward by titration with rate of reward." Behav Neurosci **105**(6): 913-25.

Gallistel, C. R., M. Leon, et al. (1996). "Destruction of the medial forebrain bundle caudal to the site of stimulation reduces rewarding efficacy but destruction rostrally does not." Behav Neurosci **110**(4): 766-90.

Gallistel, C. R., M. Leon, et al. (1991). "Effect of current on the maximum possible reward." Behav Neurosci **105**(6): 901-12.

Gallistel, C. R., P. Shizgal, et al. (1981). "A portrait of the substrate for self-stimulation." Psychol Rev **88**(3): 228-73.
Garris, P. A., M. Kilpatrick, et al. (1999). "Dissociation of dopamine release in the nucleus accumbens from intracranial self-stimulation." Nature **398**(6722): 67-9.
Guzowski, J. F., J. A. Timlin, et al. (2005). "Mapping behaviorally relevant neural circuits with immediate-early gene expression." Curr Opin Neurobiol **15**(5): 599-606.
Hartigan, J. A. H. a. P. M. (1985). "The Dip Test of Unimodality." Annals of Statistics **13**: 70-84.
Herrnstein, R. J. (1974). "Formal properties of the matching law." J Exp Anal Behav **21**(1): 159-64.
Hyder, F., D. L. Rothman, et al. (2002). "Total neuroenergetics support localized brain activity: implications for the interpretation of fMRI." Proc Natl Acad Sci U S A **99**(16): 10771-6.
Jezzard, P., P. M. Matthews, et al. (2001). Functional MRI : an introduction to methods. Oxford ; New York, Oxford University Press.
Kim, S. G. and K. Ugurbil (2003). "High-resolution functional magnetic resonance imaging of the animal brain." Methods **30**(1): 28-41.
Kita, J. M., L. E. Parker, et al. (2007). "Paradoxical modulation of short-term facilitation of dopamine release by dopamine autoreceptors." J Neurochem **102**(4): 1115-24.
Koob, G. F., H. T. Le, et al. (1987). "The D1 dopamine receptor antagonist SCH 23390 increases cocaine self-administration in the rat." Neurosci Lett **79**(3): 315-20.
Lee, A. T., G. H. Glover, et al. (1995). "Discrimination of large venous vessels in time-course spiral blood-oxygen-level-dependent magnetic-resonance functional neuroimaging." Magn Reson Med **33**(6): 745-54.
Logothetis, N. K. (2003). "The underpinnings of the BOLD functional magnetic resonance imaging signal." J Neurosci **23**(10): 3963-71.
Logothetis, N. K., J. Pauls, et al. (2001). "Neurophysiological investigation of the basis of the fMRI signal." Nature **412**(6843): 150-7.
May, L. J. and R. M. Wightman (1989). "Effects of D-2 antagonists on frequency-dependent stimulated dopamine overflow in nucleus accumbens and caudate-putamen." J Neurochem **53**(3): 898-906.
Menon, R. S. (2002). "Postacquisition suppression of large-vessel BOLD signals in high-resolution fMRI." Magn Reson Med **47**(1): 1-9.
Meredith, G. E., P. Ypma, et al. (1995). "Effects of dopamine depletion on the morphology of medium spiny neurons in the shell and core of the rat nucleus accumbens." J Neurosci **15**(5 Pt 2): 3808-20.
Murray, B. and P. Shizgal (1996). "Behavioral measures of conduction velocity and refractory period for reward-relevant axons in the anterior LH and VTA." Physiol Behav **59**(4-5): 643-52.

Nicola, S. M. and R. C. Malenka (1997). "Dopamine depresses excitatory and inhibitory synaptic transmission by distinct mechanisms in the nucleus accumbens." J Neurosci **17**(15): 5697-710.
Nicola, S. M., J. Surmeier, et al. (2000). "Dopaminergic modulation of neuronal excitability in the striatum and nucleus accumbens." Annu Rev Neurosci **23**: 185-215.
Nieuwenhuys, R., L. M. Geeraedts, et al. (1982). "The medial forebrain bundle of the rat. I. General introduction." J Comp Neurol **206**(1): 49-81.
O'Donnell, P., J. Greene, et al. (1999). "Modulation of cell firing in the nucleus accumbens." Ann N Y Acad Sci **877**: 157-75.
Ogawa, S., T. M. Lee, et al. (1990). "Brain magnetic resonance imaging with contrast dependent on blood oxygenation." Proc Natl Acad Sci U S A **87**(24): 9868-72.
Olds, J. and P. Milner (1954). "Positive reinforcement produced by electrical stimulation of septal area and other regions of rat brain." J Comp Physiol Psychol **47**(6): 419-27.
Olds, M. E. and J. Olds (1969). "Effects of lesions in medial forebrain bundle on self-stimulation behavior." Am J Physiol **217**(5): 1253-64.
Paxinos, G. (2004). The rat nervous system. Amsterdam ; Boston, Elsevier Academic Press.
Paxinos, G. and C. Watson (2007). The rat brain in stereotaxic coordinates. Amsterdam ; Boston ;, Academic Press/Elsevier.
Pennartz, C. M., H. J. Groenewegen, et al. (1994). "The nucleus accumbens as a complex of functionally distinct neuronal ensembles: an integration of behavioural, electrophysiological and anatomical data." Prog Neurobiol **42**(6): 719-61.
Pessiglione, M., B. Seymour, et al. (2006). "Dopamine-dependent prediction errors underpin reward-seeking behaviour in humans." Nature **442**(7106): 1042-5.
Porrino, L. J., R. U. Esposito, et al. (1984). "Metabolic mapping of the brain during rewarding self-stimulation." Science **224**(4646): 306-9.
Quintana, J., J. Yajeya, et al. (1988). "Prefrontal representation of stimulus attributes during delay tasks. I. Unit activity in cross-temporal integration of sensory and sensory-motor information." Brain Res **474**(2): 211-21.
Roitman, M. F., G. D. Stuber, et al. (2004). "Dopamine operates as a subsecond modulator of food seeking." J Neurosci **24**(6): 1265-71.
Schultz, W. (1999). "The Reward Signal of Midbrain Dopamine Neurons." News Physiol Sci **14**: 249-255.
Schultz, W. (2002). "Getting formal with dopamine and reward." Neuron **36**(2): 241-63.
Schultz, W., P. Dayan, et al. (1997). "A neural substrate of prediction and reward." Science **275**(5306): 1593-9.

Sharp, F. R., S. M. Sagar, et al. (1993). "Metabolic mapping with cellular resolution: c-fos vs. 2-deoxyglucose." Crit Rev Neurobiol **7**(3-4): 205-28.

Shizgal, P. (1997). "Neural basis of utility estimation." Curr Opin Neurobiol **7**(2): 198-208.

Shizgal, P., C. Bielajew, et al. (1980). "Behavioral methods for inferring anatomical linkage between rewarding brain stimulation sites." J Comp Physiol Psychol **94**(2): 227-37.

Simmons, J. M., R. F. Ackermann, et al. (1998). "Medial forebrain bundle lesions fail to structurally and functionally disconnect the ventral tegmental area from many ipsilateral forebrain nuclei: implications for the neural substrate of brain stimulation reward." J Neurosci **18**(20): 8515-33.

Simmons, J. M. and C. R. Gallistel (1994). "Saturation of subjective reward magnitude as a function of current and pulse frequency." Behav Neurosci **108**(1): 151-60.

Sokoloff, L., M. Reivich, et al. (1977). "The [14C]deoxyglucose method for the measurement of local cerebral glucose utilization: theory, procedure, and normal values in the conscious and anesthetized albino rat." J Neurochem **28**(5): 897-916.

Swanson, L. W. (1982). "The projections of the ventral tegmental area and adjacent regions: a combined fluorescent retrograde tracer and immunofluorescence study in the rat." Brain Res Bull **9**(1-6): 321-53.

Waraczynski, M., M. Perkins, et al. (1999). "Lesions of midline midbrain structures leave medial forebrain bundle self-stimulation intact." Behav Brain Res **103**(2): 175-84.

Waraczynski, M., J. R. Stellar, et al. (1987). "Reward saturation in medial forebrain bundle self-stimulation." Physiol Behav **41**(6): 585-93.

Waraczynski, M., M. N. Ton, et al. (1990). "Failure of amygdaloid lesions to increase the threshold for self-stimulation of the lateral hypothalamus and ventral tegmental area." Behav Brain Res **40**(2): 159-68.

Wise, R. A. (1982). "Neuroleptics and operant behavior: The anhedonia hypothesis." Behavioral and Brain Sciences **9**: 39-53.

Wise, R. A. and P. P. Rompre (1989). "Brain dopamine and reward." Annu Rev Psychol **40**: 191-225.

Wise, R. A., J. Spindler, et al. (1978). "Neuroleptic-induced "anhedonia" in rats: pimozide blocks reward quality of food." Science **201**(4352): 262-4.

Yang, C. R. and G. J. Mogenson (1984). "Electrophysiological responses of neurones in the nucleus accumbens to hippocampal stimulation and the attenuation of the excitatory responses by the mesolimbic dopaminergic system." Brain Res **324**(1): 69-84.

Yeomans, J. S. (1989). "Two substrates for medial forebrain bundle self-stimulation: myelinated axons and dopamine axons." Neurosci Biobehav Rev **13**(2-3): 91-8.

Yeomans, J. S., A. Mathur, et al. (1993). "Rewarding brain stimulation: role of tegmental cholinergic neurons that activate dopamine neurons." Behav Neurosci **107**(6): 1077-87.

Yim, C. Y. and G. J. Mogenson (1982). "Response of nucleus accumbens neurons to amygdala stimulation and its modification by dopamine." Brain Res **239**(2): 401-15.

Yokel, R. A. and R. A. Wise (1975). "Increased lever pressing for amphetamine after pimozide in rats: implications for a dopamine theory of reward." Science **187**(4176): 547-9.

Zahm, D. S. (1999). "Functional-anatomical implications of the nucleus accumbens core and shell subterritories." Ann N Y Acad Sci **877**: 113-28.